Preconcentration and Atomic Spectrometric Determination of Rare Earth Elements (REEs) in Environmental Samples

By

Türker PASİNLİ

**A Dissertation Submitted to the
Graduate School in Partial Fulfillment of the
Requirements for the Degree of**

MASTER OF SCIENCE

**Department: Chemistry
Major: Chemistry**

**İzmir Institute of Technology
İzmir, Turkey**

July, 2004

We approve the thesis of **Türker PASİNLİ**

Date of Signature

…….. **30.07.2004**

Assoc. Prof. Dr. Ahmet E. EROĞLU

Supervisor

Department of Chemistry

……..... **30.07.2004**

Prof. Dr. Emür HENDEN

Ege University,

Faculty of Science, Department of Chemistry

…….. **30.07.2004**

Assist. Prof. Dr. Talal SHAHWAN

Department of Chemistry

…….. **30.07.2004**

Assist. Prof. Dr. Durmuş ÖZDEMİR

Department of Chemistry

…….. **30.07.2004**

Assist. Prof. Dr. Ritchie Curtis EANES

Department of Chemistry

…….. **30.07.2004**

Prof. Dr. Levent ARTOK

Head of Chemistry Department

ACKNOWLEDGEMENTS

I would like to express sincere gratitude to my advisor, Assoc. Prof. Ahmet EROĞLU, for him supervision, guidance, support, and encouragement. I also would like to thank Assist. Prof. Talal SHAHWAN for his recommendations.

I would like to thank research specialists Oya ALTUNGÖZ and Nesrin GAFFAROĞULLARI for their contributions during the ICP-OES analyses. Also I deeply appreciate the support of my roommates, and the following research assistants: Öznur KAFTAN, Betül ÖZTÜRK, Bahar ÖZMEN, Mustafa AYDIN, Aytaç ŞAHİN, Tarık KIŞLA, and Aslı ERDEM.

Finally, I would like to thank my family for their support, encouragement, and understanding.

ABSTRACT

Determination of rare earth elements (REEs) in environmental samples is usually performed by the plasma techniques, inductively coupled plasma optical emission spectrometry (ICP-OES) and inductively coupled plasma mass spectrometry (ICP-MS). Due to low concentrations of REEs and usually the presence of heavy matrix, an efficient separation and preconcentration technique is required prior to instrumental measurements in order to achieve accurate and reliable results.

In this study, different types of zeolites (Clinoptilolite, Mordenite, Zeolite Y, Zeolite Beta), ion exchangers (Amberlite CG-120, Amberlite IR-120, Rexyn 101, Dowex 50W X18) and chelating resins (Muromac, Chelex 100, Amberlite IRC-718) were proposed as adsorbent materials for the preconcentration of REEs in environmental waters prior to their determination by ICP-OES. It was shown that REEs can be retained by these adsorbents quantitatively in a broad pH range (pH>4) and their desorptions from the adsorbents can be realized with acidic eluents. Of the sorbents investigated, clinoptilolite was chosen for the subsequent studies. Spike recovery tests were performed at various concentration levels in different water types including pure water, bottled drinking water, river water, sea water, and tap water, and were found to change between 85-90%.

ÖZ

Çevre örneklerindeki nadir toprak element tayinleri genellikle plazma teknikleri (endüktif eşleşmiş plazma optik emisyon spektrometri, ICP-OES, ve endüktif eşleşmiş plazma kütle spektrometri, ICP-MS) ile gerçekleştirilmektedir. Bu elementlerin derişimlerinin çok düşük olması ve numunelerin içerdiği ağır matriks, doğru ve güvenilir sonuçlar elde etmek için enstrümantal ölçümlerden önce etkili bir matriks ayırma/ön-deriştirme işlemini gerekli kılar.

Bu çalışmada, çevre örneklerindeki nadir toprak elementlerinin ICP-OES ile tayininden önce ön-deriştirilmeleri için çeşitli zeolitler (clinoptilolite, mordenite, zeolite Y, zeolite Beta), iyon değiştiriciler (Amberlite CG-120, Amberlite IR-120, Rexyn 101, Dowex 50W X18) ve kelatlayıcı reçineler **(**Muromac, Chelex 100, Amberlite IRC-718) önerilmektedir. Çalışmalar, nadir toprak elementlerinin söz konusu adsorbentler tarafından geniş bir pH aralığında (pH>4) tutunduklarını ve asidik eluentlerle geri kazanılabileceklerini gösterdi. Takip eden çalışmalarda clinoptilolite kullanıldı. Saf su, şişelenmiş içme suyu, nehir suyu, deniz suyu ve çeşme suyu gibi çeşitli su örneklerine değişen derişimlerde katımlarla gerçekleştirilen geri kazanım testlerinde % 85-90 arasında değişen değerler elde edildi.

TABLE OF CONTENTS

LIST OF FIGURES

LIST OF TABLES

CHAPTER 1

RARE EARTH ELEMENTS (REEs)

1.1. Introduction to Rare Earth Elements (REEs)

The term rare earth was suggested by Johann Gadolin in 1794. "Rare" because when the first of the REEs was discovered they were thought to be present in the earth's crust only in small amounts, and "earths" because as oxides they have an earthy appearance. Because of chemical similarities among the REEs, their complete isolation and classification took more than a century from their discovery (Evans 1997).

The REEs lie in the last rows of Mendeleev's periodic table, comprising both lanthanide and actinide series (Figure 1.1). The REE term is mostly employed in chemistry as a synonym of the lanthanide series. The REEs have similar physicochemical properties, which change periodically with the atomic number. They range from La to Lu (atomic numbers between 57 and 71: lanthanum (La), cerium (Ce), praseodymium (Pr), neodymium (Nd), promethium (Pm), samarium (Sm), europium (Eu), gadolinium (Gd), terbium (Tb), dysprosium (Dy), holmium (Ho), erbium (Er), thulium (Th), ytterbium (Yb), and lutetium (Lu). Yttrium (atomic number 39) a Group IIIB transition metal, although not a lanthanide is generally included with the REEs as it occurs with them in natural minerals and has similar chemical properties. For the same reason, scandium (atomic number 21) is also included with the REEs. The REEs are usually divided into three groups: light REEs, from La to Pm, the medium REEs, from Sm to Ho, and the heavy REEs, from Er to Lu.

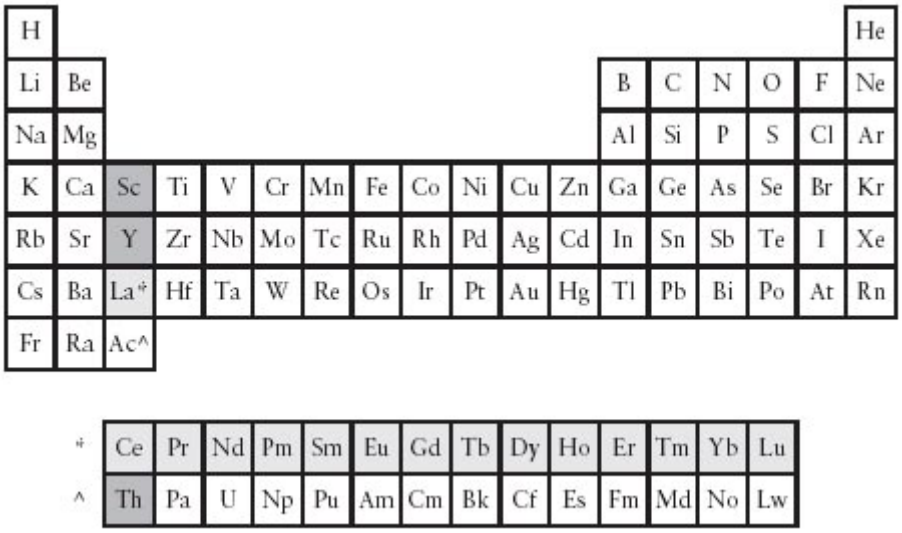

Figure 1.1. Periodic table with REEs and scandium, yttrium and thorium.

Although lanthanides are termed rare-earth elements, they are not rare in nature. Their levels in the earth's crust are often equal to or higher than some physiologically significant elements, such as iodine, cobalt, silver, gold, platinum and selenium (Brzyska 1996). Cerium (68 mg/kg) and lanthanum (32 mg/kg) are the most common. Lutetium and thulium are the rarest (about 0.5 mg/kg) while the concentrations of the remainder range from 1 to 9 mg/kg. Promethium is an artificial radioactive element with no stable isotopes.

The REEs have similar chemical and physical properties and behave relatively coherently as a group. Chemically, REEs are strong reducing agents and their compounds are generally ionic. REEs are never found as free metals in the earth's crust. All their naturally occurring minerals consist of mixtures of various REEs and nonmetals. Bastnaesite [(Ce,La)(CO_3)F], monazite [(Ce,La,Nd,Th)(PO_4)] [(REE)PO_4] and xenotime [YPO_4] are the three most significant minerals of REEs. The REEs are definitely electropositive metals with the oxidation number of +3. Only cerium, terbium and praseodymium with an oxidation number of +4 and samarium, europium and ytterbium with the oxidation number of +2 form stable compounds. Europium and cerium are the most reactive elements of the REEs (Evans 1997).

1.2. Uses of Rare Earth Elements

Lanthanide compounds frequently have magnetic, catalytic and optic properties and therefore are widely used in industry. Their industrial uses are outlined in Table 1.1.

Table 1.1. Industrial uses of REEs (Pedreira et al. 2002)

Element	Application
Lanthanum	Ceramic glazes, high quality optical glass, camera lenses, microwave crystals, ceramic capacitors, glass polishing, petroleum cracking.
Cerium	Glass polishing, petroleum cracking catalysts, alloys - with iron for sparking flints for lighters, with aluminum, magnesium and steel for improving heat and strength properties, radiation shielding, many others.
Praseodymium	Yellow ceramic pigments, tiles, ceramic capacitors. With neodymium in combination for goggles to shield glass makers against sodium glare, permanent magnets, cryogenic refrigerant.
Neodymium	Ceramic capacitors, glazes and colored glass, lasers, high strength permanent magnets as neodymium-iron-boron alloy, petroleum cracking catalysts.
Promethium	Radioactive promethium in batteries to power watches, guided missile instruments, etc, in harsh environments.
Samarium	In highly magnetic alloys for permanent magnet as samarium-cobalt alloy; probably will be superseded by neodymium. Glass lasers. Reactor control and neutron shielding.
Europium	Control rods in nuclear reactors. Colored lamps, cathode ray tubes. Red phosphor in colour television tubes.

(Table 1 cont. on next page)

Table 1. (continued)

Gadolinium	Solid state lasers, constituent of computer memory chips, high temperature refractories, cryogenic refrigerants.
Terbium	Cathode ray tubes, magnets, optical computer memories; future hard disk components; magnetostrictive alloys.
Dysprosium	Controls nuclear reactors. Alloyed with neodymium for permanent magnets. Catalysts.
Holmium	Controls nuclear reactors; catalysts; refractories.
Erbium	In ceramics to produce a pink glaze; infra-red absorbing glasses.
Thulium	X-ray source in portable X-ray machines.
Ytterbium	Practical values presently unknown. Research.
Lutetium	Deoxidiser in stainless steel production, rechargeable batteries, medical uses, red phosphors for color television, superconductors.
Yttrium	Deoxidiser in stainless steel production, rechargeable batteries, medical uses, red phosphors for color television, superconductors.
Scandium	X-ray tubes, catalysts for polymerization, hardened Ni-Cr super alloys, dental porcelain.

In the last twenty years new technologies have been introduced in metallurgical, optical and electronic industries, which increased the role of artificial lanthanide compounds with special physicochemical properties. At present, metallurgy utilizes about 37% of lanthanides and their compounds which is used to remove oxygen and to enrich steel. Thirty percent of lanthanides are used for catalytic converters, 29% in ceramic industry, and 1% in other industries. Pure lanthanide compounds are used in electronics and optoelectronics to produce luminophores (oxides of lanthanum, gadolinium, europium and terbium), lasers (e.g., halogens of neodymium, holmium and erbium), optical fibers, components of magnetic memories (e.g., gadolinium-gallium garnet, GGG), permanent magnets (alloys of samarium and neodymium) and high-temperature superconductors. Also they are used as magnetic resonance imaging (MRI)

contrast reagents in medicine, and also lanthanum chloride ($LaCl_3$) is added to chemical fertilizers in China (Liang et al. 1991, Gorbunov et al.1992, Sloof et al. 1993, Brzyska 1996, Evans 1997, Shuai et al. 2000, Liang et al. 2001).

1.3. Biological Effects of Rare Earth Elements

Rare earth elements are released into the environment as a result of their industrial uses (Gorbunov et al. 1992). Continuous exposure to low concentrations of REEs could cause adverse health effects because of their bioaccumulation along the food chain. Although there is so far no reported incidence of intoxication due to the intake of REEs through the food chain, several deleterious effects due to occupational and environmental exposure to REEs have been reported (Sabbioni et al.1982, Sax 1984). According to these reports, rare earth elements have both positive and negative effects on human health. For example rare earth elements show benefit in the liver where gadolinium selectively inhibits secretion by Kupffer cells and decrease cytochrome P450 activity in hepatocytes, thereby protecting liver cells against toxic products of xenobiotic biotransformation. Praseodymium ion (Pr^{3+}) produces the same protective effect in liver tissue cultures. On the other hand, cytophysiological effects of lanthanides appear to result from the similarity of their cationic radii to the size of Ca^{2+} ions, their high degree of ionic bonding and their donor atom affinities. Trivalent lanthanide ions, especially La^{3+} and Gd^{3+}, block different calcium channels in human and animal cells. Lanthanides can affect numerous enzymes. Dy^{3+} and La^{3+} block Ca^{2+}-ATPase and Mg^{2+}-ATPase, while Eu^{3+} and Tb^{3+} inhibit calcineurin. In neurons, lanthanide ions regulate the transport and release of synaptic transmitters and block some membrane receptors, e.g. GABA and glutamate receptors (Palasz et al.2000).

It is likely that lanthanides significantly and uniquely affect biochemical pathways, thus altering physiological processes in the tissues of humans and animals.

1.4. Determination of Rare Earth Elements

As the demand for high purity rare earth compounds is increasing and for environmental protection, the development of new precise and accurate analytical methods for the determination of REEs is required at trace levels.

For many years, the most common analytical techniques for measuring REEs have been neutron activation analysis (NAA) (Orvini et al. 2000, Figueiredo et al. 2002, Minowa et al. 2003) and isotope dilution mass spectrometry (IDMS) (Hoyle et al. 1983, Greaves et al. 1989, and Noemia et al. 1990). These methods are, however, time consuming and require very sophisticated equipment, unviable to most laboratories. The inductively coupled plasma optical emission spectrometry (ICP-OES) is one of the most effective multi-element techniques for the quantitative determination of many trace elements with widely varying matrices, and is often used in the determination of the REEs. Instrumental detection limits are stated to be on the order of 50.0 μg/L (Djingova et al. 2002). The more recent inductively coupled plasma mass spectroscopy (ICP-MS) technique is a powerful method for the direct determination of REEs (detection limits, in the order of 2.0 μg/L (Pedreira et al. 2002), but the equipment is still too expensive for many laboratories.

1.4.1. Inductively Coupled Plasma Optical Emission Spectrometry (ICP-OES)

Inductively coupled plasma optical emission spectrometry (ICP-OES) is an important analytical tool in a wide range of scientific disciplines. It is used for simultaneous determination of over 70 elements in virtually any sample in less than 2 minutes. Concentrations from parts per billion to weight % can be determined without preconcentration or dilution**.** The ICP-OES method enables multi-element determination with high levels of precision and accuracy for most elements (<1% RSD). Also it offers low detection limits, rapid analytical procedure, a large dynamic range (four or more orders of magnitude), and complete removal of the analyte from its original matrix in order to minimize interferences with lower matrix background (Settle 1997).

ICP-OES is based on the fact that atoms are promoted to higher electronic energy levels when heated to high temperatures. In fact, the plasma temperature is sufficient to ionize most atoms. For about three-quarters of the elements amenable to

the technique, the most sensitive line arises from an ion rather than an atom. As the excited species leave the high-temperature region, the absorbed energy is released as ultraviolet and visible photons when the excited atoms decay to lower energy levels or the ground electronic state. Useful emission lines generally occur in the region between 160 and 900 nm. Atomic and ionic emission lines are very narrow, typically less than 5 pm, and their wavelengths follow well-understood selection rules (Settle 1997).

The ICP is estimated to produce a typical temperature of 6500 ^{0}K and this high temperature is sufficient to break virtually all chemical bonds in a sample. Consequently, the emitting atoms and ions are virtually independent of one another. As a result, the technique exhibits high sensitivity, a linear range of four or more orders of magnitude, and much reduced chemical interference relative to AAS or arc/spark emission techniques (Settle 1997).

In an ICP-OES determination, the samples are most commonly introduced into the plasma as aerosols. A wide variety of devices are available for sample introduction. Pneumatic nebulizers are the least expensive and most commonly used in commercial devices. The aerosol produced by the nebulizer is generally passed through a spray chamber to remove large droplets and produce a more homogeneous aerosol. While passing through the plasma, the aerosol is vaporized, atomized, perhaps ionized, and then electronically excited. After leaving the plasma, the sample emits photons, which are sampled through a narrow entrance slit and dispersed with grating monochromotor. The resolved radiations are measured with a photomultiplier tube or array detectors (such as a charge coupled device, CCD or charge injection device, CID), which converts the optical signal into an electrical signal. An electronic interface converts the signal into an appropriate form for measurement and storage by a dedicated computer (Settle 1997).

ICP-OES has been widely used in the determination of trace REEs. For example; Liang et al. (2001) used ICP-OES for the determination of La, Y, Yb, Eu, Dy after preconcentration step with nanometer-sized titanium dioxide micro-column. The technique was used by Shuai et al. (2000) for the determination of rare earth impurities in high-purity lanthanum oxide, by Iwasaki (1986) and Rucandio (1992) for the determination of lanthanides and yttrium in rare earth ores; and by Crock et al. (1982) for determination of rare earth elements in geological materials.

1.4.2. Preconcentration and Separation of Rare Earth Elements

Inductively coupled plasma optical emission spectrometry, as mentioned, offers one of the most suitable techniques for REEs determination. However, the low level of REEs in samples is not compatible with the detection limits exhibited by this technique. Also major constituents, such as organic compounds and inorganic salts, cause matrix effects. In order to achieve accurate and reliable results, efficient preconcentration of REEs and their separation from matrix is required.

One of the most widely used techniques for the separation and preconcentration of trace REEs has been co-precipitation. For example, Roychowdhury et al. (1989) precipitated REEs and Y as oxalates using calcium as a carrier. In another study Greaves et al. (1989) employed a precipitation step with hydrated iron (III) oxide followed by a purification procedure using a single cation-exchange column after which the sorbed species were eluted with hydrochloric and nitric acids. Liquid-liquid extraction is another efficient separation technique used in the studies related with REEs. Wang et al. (2004) applied the technique in the separation of Y from heavy REEs using a novel organic carboxylic acid, *s*-Nonylphenoxy acetic acid, as extractant in the presence of several other complexing agents such as EDTA, DTPA, or HEDTA. Ion exchange procedures have also been applied successfully for the separation of REEs from geological materials [Navarro et al. 2002]. In this study, the researchers separated REEs with a cation exchange resin; then they eluted the sorbed species with a nitric acid-oxalic acid mixture. Zhu et al. (1998) utilized an ion-exchange microcolumn prepared with Diol silica consisting of a acrylic acid/acrylamide copolymer. Elution of REEs from the microcolumn was realized with 0.25 M HNO_3. Möller et. al (1992) used Chelex 100 chelating resin for preconcentration of REEs in sea water by ion exchange chromatography. High performance liquid chromatography (HPLC) was also applied in the determination of REEs. In one such study, Qin et al. (2000) used a 2-ethylhexylhydrogen 2-ethylhexylphosphonate resin as the stationary phase and dilute nitric acid as the mobile phase for the separation of REE impurities in high purity cerium oxide.

1.4.2.1. Solid-Phase Extraction (SPE)

In addition to the preconcentration / separation techniques mentioned above, the solid-phase extraction (SPE) technique has become increasingly popular in recent years (Grebneva et al. 1996, Vicente et al. 1998, Dev et al. 1999, Liang et al. 2001, Hirata et al. 2002). It is an extraction method that uses a solid phase and a liquid phase to isolate one, or one type, of analyte from a solution. It is usually used to clean up a sample before using a chromatographic or other analytical method to quantitate the amount of analyte(s) in the sample. The solid phase extraction technique has several advantages; (i) it is simple to implement, (ii) high preconcentration factors can be obtained by SPE , (iii) it enables rapid phase separation, and (iv) it can be combined with different techniques. The general procedure is to load a solution onto the SPE phase, wash away undesired components, and then wash off the desired analytes with another solvent into a collection tube.

The solid phase extraction method is widely used in chromatographic preconcentration studies that can be performed in two distinct forms, the batch and the column methods. In our project we used the batch method. In the batch mode, a quantity of the chromatographic stationary phase (or sorbent) is added to the sample and the mixture is then shaken for some time. If the conditions are suitable, the analytes of some interest become bound to the sorbent and are then separated from the sample solution by filtration.

Column preconcentration can be performed either off-line or on-line. In the former case, the sample is passed through a suitable column after which the enriched analyte is desorbed from the column and the resultant solution is analyzed by an appropriate procedure. In the on-line method, the sorbent column is coupled directly to the analytical instrument so that the sample enrichment, desorption, and analysis steps can be carried out at the same run automatically.

1.5. Aim of This Work

The purpose of this study is to develop a sensitive enrichment/matrix separation procedure for the determination of REEs in environmental water samples. For this purpose, several cation exchangers (Amberlite CG-120, Amberlite IR-120, Rexyn 101, Dowex 50W X18), chelating resins **(**Muromac, Chelex 100, Amberlite IRC-718) and zeolites (clinoptilolite, mordenite, zeolite Y, zeolite Beta) were tried and the natural zeolite, clinoptilolite, was suggested as a proper sorbent for subsequent studies. The efficiency of clinoptilolite was evaluated through preconcentration and recovery studies. Determination of REEs concentrations were obtained by (ICP-OES).

CHAPTER 2

ZEOLITES AND SORPTION

2.1. Introduction to Zeolites

Zeolite is the crystalline, hydrated aluminosilicate of alkaline or alkaline earth metals, especially, sodium, potassium, calcium, magnesium, strontium and barium. Structurally, zeolite is the "framework" aluminosilicate composed of an infinitely extended three-dimensional network of AlO_4 and SiO_4 tetrahedra that form channels and interconnected voids, which are occupied by cations and water molecules. It may be expressed as two different formulas, an oxide formula and an idealized formula represented as follows:

- Oxide formula: $M_{2/n}O.Al_2O_3.xSiO_2.yH_2O$
- Idealized formula: $M_{x/n}[(AlO_2)_x(SiO_2)_y].wH_2O$

In the oxide formula, M represents the cation of valence, n for the idealized formula and x is generally equal to or greater than 2 since AlO_4 tetrahedra can join only to SiO_4 tetrahedra. The structural formula of a zeolite may be best expressed by the idealized formula for the crystallographic unit cell where w is the number of water molecules and the ratio y/x varies between 1 and 5 depending on the structure. The sum (x + y) represents the total number of tetrahedra, while the portion within brackets [..] defines the framework composition. (Breck 1974, Tsitsishvili et al. 1992).

The primary building unit of the zeolite framework is the tetrahedron in which the center is occupied by a silicon or aluminum atom with four oxygen atoms at the corners as shown in Figure 2.1. Each oxygen atom is shared between two tetrahedra. Hence, the tetrahedra form a continuous framework. Substitution of Si^{4+} by Al^{3+} defines the negative charge of framework, which is compensated by monovalent or divalent cations

located together with water molecules in the channels. Cations in the channels can be substituted easily and therefore, they are termed exchange or extra framework cations, while Si and Al, which are not exchanged under ordinary conditions, are called tetrahedral (T) or framework cations. (Tsitsishvili et al. 1992)

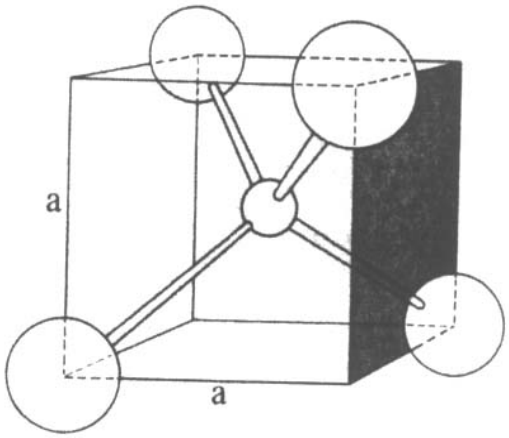

Figure 2.1. $(SiO_4)^{4-}$ or $(AlO_4)^{4-}$ tetrahedron

A zeolite structure can be summarized as having an aluminosilicate framework, exchangeable cations and zeolitic water. The aluminosilicate framework is the most stable component and defines the structure. Exchangeable cations are surrounded by water molecules and oxygen atoms fill the channels and cavities in the zeolite framework charge, acting as a stabilizer. (Tsitsishvili et al. 1992)

Zeolites have superior characteristics compared to the other crystalline inorganic oxide-materials. For example; they can separate molecules based on the size and configuration of the molecule relative to the size and geometry of the apertures of the zeolite structure, due to the uniform and microporous pore structure within their crystals. Thus, they act as “molecular sieves”. They also adsorb molecules which have a permanent dipole moment with selectivity not found in other adsorbents. (Breck 1974, Moscou 1991) Zeolites are accessible to perform all sorts of ion exchange reactions. They are suitable for catalyzing organic reactions because of their high thermal stability and internal acidity.

Since all metal-oxygen tetrahedra are exposed to the internal zeolite surface, they are in principle all accessible depending on pore dimensions. This makes zeolites

appropriate for all sorts of modifications. These modifications are exchange of extra-framework cations, replacement of tetrahedral cations, and introduction of metal particles.

2.2 Clinoptilolite (A Natural Zeolite)

Clinoptilolite, a member of the heulandite group of natural zeolites, is the most abundant zeolite found in nature (Gottardi and Galli 1985, Tsitsishvili et al. 1992). Its approximate chemical composition may be expressed as follows (Tsitsishvili et al. 1992)

- Oxide formula: $(K, Na, 1/2Ca)_2\,O.Al_2O_3.10SiO_2.8H_2O$
- Idealized formula: $(K_2, Na_2, Ca)_3\,[(Al_{16}\,Si_{30})O_{72}].24H_2O$

However, there may be remarkable changes in the composition of the framework and exchangeable cations. K^+, Na^+, Ca^{2+}, and Mg^{2+} are the most common charge-balancing cations. Small but measurable amounts of Fe^{3+} may be found in clinoptilolite mineral (Ackley et al. 1992).

Clinoptilolite is isostructural with heulandite (i.e. they both have same XRD patterns). Yet, there exist some differences between them. Clinoptilolite has Si/Al>4, while heulandite, contains Si/Al<4. As a result of its high Si/Al ratio, clinoptilolite is thermally stable to temperatures in excess of 500 ^{0}C, as opposed to heulandite which undergoes structural collapse at 350 ^{0}C because bonds between Si and O are much stronger than Al-O bonds (Zhao et al. 1998). On the other hand, lower Al content of the clinoptilolite brings about low cation density, 3 bivalent cations or 6 monovalent cations per unit cell at maximum (Tsitsishvili et al. 1992). Clinoptilolite can also be distinguished from heulandite on the basis of cation content, where alkali cations dominant [(Na+K)>Ca], whereas heulandite has Ca>(Na+K). Finally, clinoptilolite generally contains somewhat less water than heulandite (Smyth et al. 1990).

2.2.1. Structure of Clinoptilolite

It has been stated that, cation exchange, catalytic, and adsorption properties, behavior of zeolitic water, stability as well as various physical properties such as electrical conductivity are strongly based on the structure of clinoptilolite(Breck 1974). Thus, in order to interpret and relate these properties, structural information is essential.

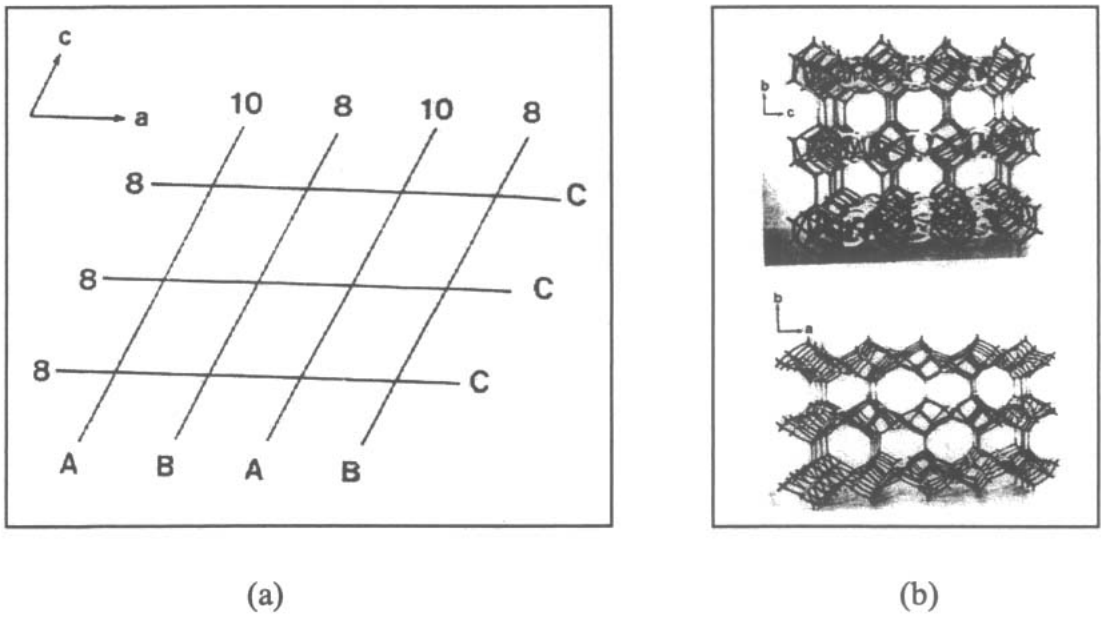

Figure 2.2. a) Orientation of clinoptilolite channel axis; **b)** Model framework for the structure of clinoptilolite. (Figure taken from Ackley and Yang 1991).

Clinoptilolite has a heulandite topology, whose secondary building unit can be described by 4-4-1 type. According to the literature (Ackley and Yang 1991), the structure of clinoptilolite consists of a two dimensional system where two types of channels, A (10-member ring) and B (8-member ring) are perpendicularly intersected by channel C (8-member ring) as shown in Figure 2.2. Channel characteristics and cation sites of clinoptilolite are summarized in Table 2.1.

Table 2.1. Channel characteristics and cation sites in clinoptilolite (Ackley and Yang 1991).

Channel	Tetrahedral ring size/channel axis	Cation Site	Major Cations	Approx. Channel dim. (nm x nm)
A	10/c	M(1)	Na, Ca	0.72 x 0.44
B	8/c	M(2)	Ca, Na	0.47 x 0.41
C	8/a	M(3)	K	0.55 x 0.40
A	10/c	M(4)	Mg	0.72 x 0.44

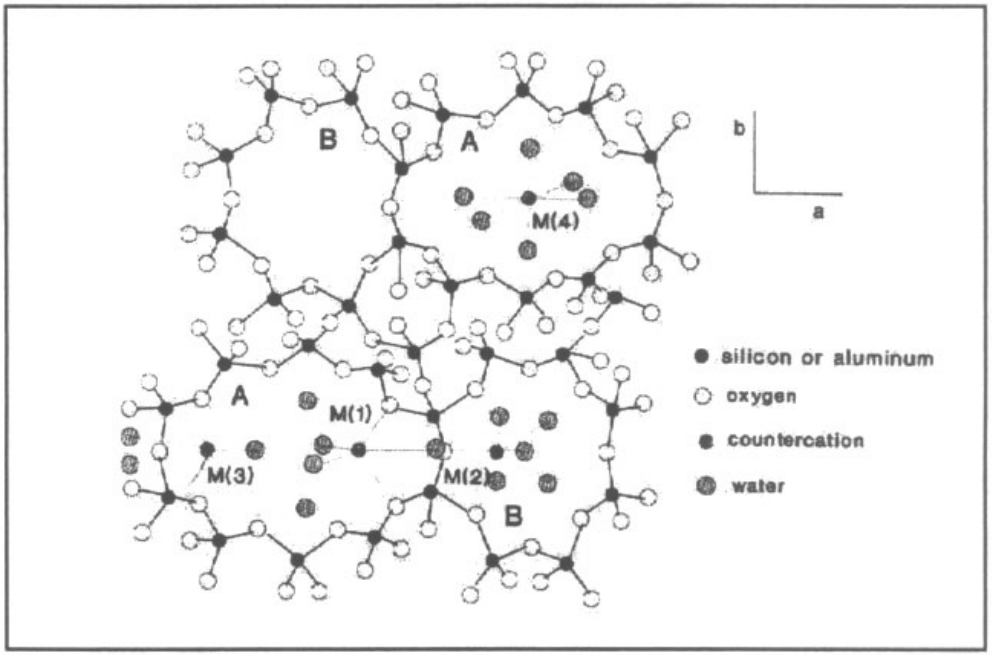

Figure 2.3. The c-axis projection of the structure of clinoptilolite (Arcoya et al. 1996)

A view of clinoptilolite structure, including the cation sites is represented in Figure 2.3. The main cation position in this structure is M(1), in channel A, which is coordinated with two framework oxygen and five H_2O molecules. This site is occupied by Ca^{2+} and preferably by Na^{+}. M(2), located in channels B is coordinated by three framework oxygen atoms and five H_2O molecules. M(2) is occupied by Na^{+} and preferably Ca^{2+}. M(3), situated in channel C, is coordinated by six framework oxygen atoms and three H_2O molecules. It is occupied by K^{+} and probably, Ba^{2+}. Because this position is very close to M(1), the simultaneous occupancy of both sites is not possible.

M(4) located in the center of channel A is different from M(1). It is coordinated by six H_2O molecules forming an octahedral system. The occupancy of this site is low, and provided by Mg^{2+} (Arcoya et al. 1996).

2.2.2. Uses of Clinoptilolite

Uses of natural clinoptilolite can be summarized as bulk mineral applications, adsorption processes and ion exchange separations. Catalytic applications are limited when compared to the synthetic zeolites.

- Clinoptilolite improves growth and feed utilization and is used to reduce disease in cattle, sheep, and chickens by addition of 1 to 5 wt. % clinoptilolite to the diet of food animals (Pond 1995).

- It improves fertilizer efficiency, reducing nitrate leaching by 30 % and increasing NH_4^+ and K^+ retention (Allen and Ming 1995).

- It improves soil physical properties and to acts as a remedy acidic or contaminated soils due to the its rigid and porous structure, chemical stability in the range of common soil pHs, physical hardness, high cation exchange capacity , and ion selectivity (Eberl et al. 1995).

- It is used in natural gas purification and drying (removal of CO_2, H_2S, N_2, and H_2O), air separation (both O_2 and N_2 production), flue gas cleanup (SO_2 removal), and NH_3 removal in coal gasification (Ackley et al. 1992).

- It is used in the treatment of municipal wastewaters, removal of ammonia, removal of cesium and strontium from radioactive wastewaters and removal of heavy metals from industrial wastewaters (Kesraoui-Ouki et al. 1994).

2.3. Sorption Isotherm Models

The equilibrium sorption data at a given temperature is usually represented by an adsorption isotherm, which is a relationship between the quantity sorbed per unit mass of solid and the concentration of the sorbate in solution. Many theoretical and empirical models have been developed to represent the various types of adsorption isotherms. The Langmuir and Freundlich models are among the most frequently used isotherm models for this purpose.

2.3.1. Langmuir Isotherm Model

A simple model of the solid surface is used to derive the equation of this isotherm. In this model, the solid is assumed to have a uniform surface at which there are no interaction between one sorbed molecule and another, the sorbed molecules are localized at specific sites and only a monolayer can be sorbed. The Langmuir isotherm is expressed as:

$$[C]_s = \frac{K.C_m.[C]_l}{1 + K.[C]_l} \qquad (2.1)$$

where:

$[C]_s$: Amount of solute per unit mass of solid phase (meq/g)

C_m : Maximum amount of solute that can be sorbed by the solid phase (meq/g)

$[C]_l$: Equilibrium concentration of solute in solution (meq/mL)

K : A constant related to the energy of sorption

The equation above may be rearranged to lead to the linear form:

$$[C]_s = C_m - \frac{[C]_s}{K.[C]_l} \qquad (2.2)$$

By plotting $[C]_s$ versus $[C]_s/[C]_l$, a straight line is obtained. The slope of that line gives "1/K" and the intercept gives "C_m" (Shahwan 2000).

2.3.2. Freundlich Isotherm Model

The Freundlich Isotherm Model is the most widely used non-linear model for describing the dependence of sorption on adsorbate concentration. The general expression of Freundlich isotherm is given as:

$$[C]_s = k\,[C]_l^n \qquad (2.3)$$

where:

$[C]_s$: the amount of ions adsorbed on the solid matrix at equilibrium (meq/g)

$[C]_l$: the concentration of the cation in solution at equilibrium (meq/mL)

k and n : Freundlich constants that refer to sorption affinity and sorption linearity

This expression can be linearized as:

$$\log [C]_s = \log k + n \log [C]_l \qquad (2.4)$$

Plotting $\log [C]_s$ versus $\log [C]_l$ yields "n" as the slope and "log k" as the intercept.

The Freundlich isotherm model allows for several kinds of adsorption sites on the solid, each having a different heat of adsorption. The Freundlich isotherm represents well the data at low and intermediate concentrations and is a good model for heterogeneous surfaces. When the value of Freundlich constant *n* is equal to unity, the Freundlich equation becomes linear and the Freundlich constant k becomes equivalent to the distribution ratio, R_d which to an empirical constant usually used in the quantification of the sorption process (Shahwan 2000).

CHAPTER 3

EXPERIMENTAL

3.1. Chemicals and Reagents

All reagents were of analytical grade. Ultra pure water (18MΩ) was used throughout the study. Glassware and plasticware were cleaned by soaking them in diluted nitric acid (10% v/v) and rinsed with distilled water prior to use.

Clinoptilolite-rich natural zeolite mineral used in this study was obtained from Enli Mining Co., Gördes, Western Anatolia.

1. Standard multi-element REEs stock solution (1000 mg/L): Prepared by dissolving 0.31172 g of lanthanum nitrate $La(NO_3)_3$, 0.30996 g of cerium nitrate $[Ce(NO_3)_3.6H_2O]$, 0.2397 g of praseodymium oxide (Pr_2O_3), 0.1148 g of dysprosium oxide (Dy_2O_3), 0.11664 g of neodymium oxide (Nd_2O_3), 0.1158 g of europium oxide (Eu_2O_3), 0.11436 g of erbium oxide (Er_2O_3), 0.11528 g of gadolinium oxide (Gd_2O_3), 0.11388 g of ytterbium oxide (Yb_2O_3), 0.23524 g of terbium oxide (Tb_2O_3), and 0.11456 g of holmium oxide (Ho_2O_3) in 100 mL ultra pure water.
2. Calibration Standards: Lower concentration standards were prepared daily from multi-REEs stock standard solution.
3. pH buffers, ranging from 2 to 10, were prepared using various concentration of KHP, NaOH , HCl, $Na_2B_4O_7$, and KH_2P (analytical grade).

3.2. Apparatus

In sorption studies with the batch method, a Yellowline RS 10 orbital shaker was used to provide efficient mixing. The pH measurements were performed by using a Corning 450 pH/ion meter with a pH combination electrode.

3.3. Instrumentation

A Varian Liberty Series II ICP Axial view optical emission spectrometer was used for the measurements. The operating conditions of the instrument and the spectral lines of REEs were given in Table 3.1 and 3.2, respectively.

Table 3.1. ICP-OES instrumentation and operating conditions

Spectrometer	
Varian Liberty Series II ICP Atomic emission spectrometer (Axial view)	
Monochromator	
Czerny-Turner	0.75 meters
Grating	90x100 mm holographic
Grating density	1800 grooves/mm
Detection	
R199UH UV enhanced solar blind 175*-300 nm with Cs-Te photocathode for UV region R446 300-940 nm wide range with multi-alkali photocathode for visible region	
Plasma conditions	
40 MHz, axial view	
Incident power (kW)	1.2
Argon flow rates (L min^{-1})	
Plasma	15
Auxiliary	1.5
Nebulizer	0.75
Nebulizers	
Concentric Glass Nebulizer	
Concentric (Sturman-Masters double pass type) with cyclonic chamber	
Sample injection modes	
Continuous nebulization	
Signal processing	
Line measurement	Peak height
Background correction	Polynomial plotted background correction

Table 3.2. Spectral lines used for the determination of REE by ICP-OES (ionic lines).

Element	Spectral Line (nm)
Ce	413.380
Dy	353.170
Er	.337.276
Eu	420.505
Gd	342.247
Ho	345.600
La	.379.478
Nd	460.109
Pr	390.844
Tb	350.917
Yb	369.419

3.4. XRPD and SEM/EDS Characterization of Clinoptilolite

As it is shown later in this thesis, clinoptilolite was chosen as the appropriate sorbent for the sorption of REEs among all the sorbents tested in this work. X-ray powder diffraction (XRPD) characterization showed that the natural samples of clinoptilolite were almost pure.

Elemental content of the mineral was revealed using energy dispersive x-ray spectroscopy (EDS). The percentages of the elements are given in Table 3.3. The values given correspond to an average of 3 data points selected randomly on the surface of clinoptilolite.

A scanning electron microscope (SEM) microimage is provided in Figure 3.1. The figure shows typical clinoptilolite crystals with sizes varying up to several μm.

Table 3.3. Elemental contents of clinoptilolite

Element	Wt. %	At. %
O	47.85	63.51
Na	0.64	0.59
Mg	1.06	0.93
Al	7.34	5.75
Si	34.26	25.93
K	2.86	1.56
Ca	2.04	1.09
Ba	3.95	0.61

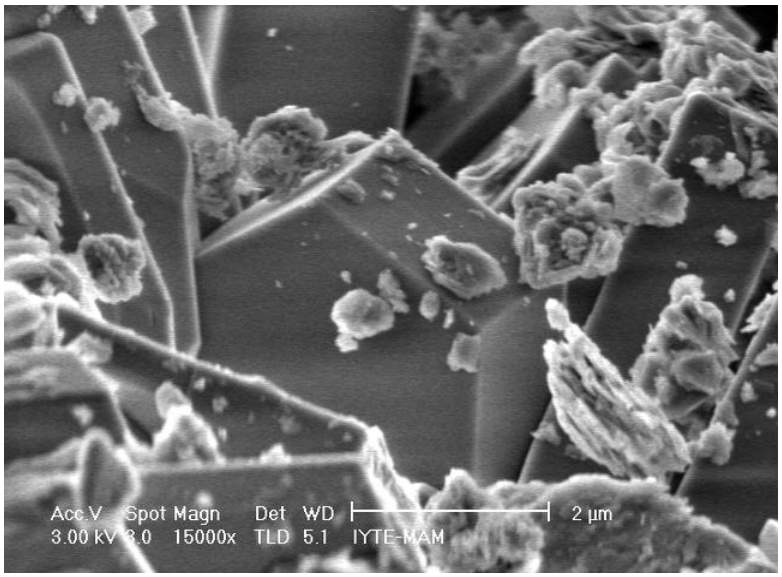

Figure 3.1. A typical SEM micrograph showing clinoptilolite crystal in the natural mineral

3.5. Determination of REEs

3.5.1. Calibration Curves for REEs

3.5.1.1. Aqueous Calibration Plot

Standard solutions from 0.01 mg/L to 2.0 mg/L were prepared from 1000 mg/L multi-element REEs standard with simple dilution. All standards contained 1% (v/v) HNO_3 corresponding to a HNO_3 molarity of 0.144M.

3.5.1.2. Matrix-Matched Calibration Plot

The matrix-matched standard graph was obtained by applying the proposed sorption/desorption steps with clinoptilolite. By the help of that method we can eliminate the suppression effect of sample pretreated and the matrix of the eluate originating from clinoptilolite. In order to plot matrix-matched calibration curves of REEs, standard solutions from 0.01 mg/L to 2.0 mg/L were mixed with clinoptilolite (0.1g). The solutions were shaken manually for 1-2 minutes and then placed on the shaker for 30 minutes at room temperature. The contents were collected on filter papers and then the sorbed species were eluted using a 2.0 M HNO_3 solution. The resultant solutions were analyzed by ICP-OES.

3.5.2. Sorption Studies

3.5.2.1. Types of Sorbents

In order to find the appropriate sorbent for the sorption of REEs, various materials such as chelating resins, cation exchangers, natural and synthetic zeolites were tried. The sorption experiments were performed with the batch method because of the small particle size of most of the materials tested. As an initial experiment, 1.0 mg/L multi-element REEs standard solution was prepared at a pH of 7. To 20.0 mL of this solution, 0.1g of the tested sorbent was added and the mixture was shaken manually for 1-2 minutes before being placed on the shaker for a further 30 minutes at room temperature. At the end of the shaking period, the mixture was filtered and filtrate was analyzed by ICP-OES for percent sorption. The sorbents used in this study are given in Table 3.4.

Table 3.4. Sorbents investigated in sorption studies

Sorbent	Type	Functional groups
Dowex 50W X18	strong cation exchanger	sulfonic acid groups
Rexyn 101	strong cation exchanger	sulfonic acid groups
Amberlite CG-120	strong cation exchanger	Na^+ form, sulfonic acid groups
Amberlite IR-120	strong cation exchanger	H^+ form, sulfonic acid groups
Amberlite IRC-718	chelating resin	Na^+ form, iminodiacetate groups
Chelex 100	chelating resin	Na^+ form, iminodiacetate groups
Muromac	chelating resin	iminodiacetate groups
Clinoptilolite	natural zeolite	not treated
Zeolite Y	synthetic zeolite	ammonium form
Zeolite Beta	synthetic zeolite	ammonium form
Mordenite	synthetic zeolite	ammonium form

3.5.2.2. Effect of pH on Sorption

To investigate the effect of pH on sorption, 1.0 mg/L multi-element REEs standard solutions were prepared in different pHs by using buffer solutions and with the HNO_3 acid concentrations at a constant ionic strength (HNO_3 concentration, 0.5-4.0 M; pH 2-10). The sorbent (0.1g) was added immediately to these solutions. The mixtures were shaken manually for 1-2 minutes and then placed on the shaker for 30 minutes at room temperature. The contents were collected on filter papers. The resultant solutions were analyzed by ICP-OES using the optimum conditions.

3.5.2.3. Effect of Shaking Time

In order to obtain quantitative sorption, the effect of shaking time was investigated. For this purpose, 20.0 mL of 1.0 mg/L multi-element REEs solutions containing 0.1 g of clinoptilolite were shaken from 1 min to 120 minutes. After filtration, the resultant solutions were made acidic (1 % HNO_3 v/v) and were analyzed by ICP-OES using the optimum conditions.

3.5.2.4. Effect of Sorbent Amount

The amount of sorbent is an important factor for quantitative sorption of the analytes from a given solution. For this purpose, 20.0 mL of 1.0 mg/L multi-element REEs solutions were shaken with varying amounts of clinoptilolite (0.02g to 0.30g) for 30 minutes. After filtration the resultant solutions were analyzed by ICP-OES.

3.5.3. Determination of Sorption Isotherms

The equilibrium sorption isotherms were conducted in batch mode at pH 7. The range of concentration of REEs solutions were varied from 0.01 to 10.0 mg/L. Twenty milliliter of these solutions were shaken with 0.1 g clinoptilolite for 30 minutes and the resultant solutions were analyzed by ICP-OES. Adsorbed metal amount per unit mass of solid was calculated from the mass balance. Equilibrium sorption isotherms were obtained by plotting of REEs sorbed per mass of solid as a function of residual concentration of REEs at equilibrium.

3.5.4. Desorption from the Sorbent (Clinoptilolite)

After collection of REEs by clinoptilolite, their release was investigated using several eluents (NaCl, KCl, and HNO_3). For this purpose, 20.0 mL of 1.0 mg/L multi-element REEs was prepared and 0.1 g of sorbent was added to it. After shaking for 30 minutes, the mixture was filtered and the sorbent together with the filter paper was taken into the desorbing solution (20.0 mL). The new mixture was shaken once again for 15 minutes. At the end of this period, the solution was filtered and the filtrate was analyzed for its REEs content.

3.5.5. Preconcentration

In order to investigate the efficiency of clinoptilolite in the enrichment of REEs, from different volumes and different concentrations, solution at various volumes (20.0-1000.0 mL) and concentrations (1.0-0.02 mg/L) were prepared in ultra pure water. Appropriate amounts of clinoptilolite (from 0.1g to 1.0g depending on the volume) were

added into each solution and the mixtures were shaken as before. After filtration the sorbent and the filter paper was put into 20.0 mL of 2.0 M HNO_3. As will be shown later, 2.0 M HNO_3 was used as the eluent for desorption. The preconcentration method proposed was also applied to the water samples including tap water, bottled drinking water, river water from near the campus and sea water from Gülbahçe Bay.

3.5.6. Method Validation

Method validation was realized through spike recovery tests with ultra pure water, tap water, bottled drinking water, river water and sea water samples. Aliquots of sample were spiked with 1.0 mg/L multi-element REEs and mixed with clinoptilolite. After the usual shaking period, the mixture was filtered and the sorbent together with the filter paper was taken into 2.0 M HNO_3 for desorption. The blank solution and the calibration standards were prepared using the same procedure. The so-called “recovered standard calibration curve” was used in quantitation. These standards prepared after sorption and elution can therefore be considered as the “matrix-matched standards”. The concentrations of REEs in the eluent were determined by ICP-OES and the percent recovery in each sample was calculated.

CHAPTER 4

RESULTS AND DISCUSSION

4.1. Determination of REEs

4.1.1. Calibration Curves for REEs

Plots of emission intensity versus concentration were constructed for all REEs using ICP-OES. These graphs can be found in Appendix A. As can be seen in these graphs, all elements showed similar responses. In this section, three selected plots are provided; Fig. 4.1 for La (as a representative of the light REEs; La, Ce, Pr, Nd, Pm), Fig. 4.2 for Eu (as a representative of the medium REEs; Eu, Gd, Tb, Dy, Ho), and Fig. 4.3 for Yb (as a representative of the heavy REEs; Er, Tm, Yb, Lu).

Although not shown in these figures, calibration plots were linear at least up to 15.0 mg/L. Since we had been working with concentrations smaller than 2.0 mg/L, only the related ranges of these calibration plots are given here. The limit of detection (LOD) values based on 3s (3 times the standard deviation above the blank value) were very similar and ranged between 0.0002 and 0.0006 mg/L for the studied REEs.

In the recovery studies, various concentration in the linear dynamic range were prepared and subjected to the same sorption and desorption process with the optimized conditions (20.0 mL standard at a neutral pH, addition of 0.1 g clinoptilolite, shaking both manually and on a shaker for 30 minutes, filtration, desorption of REEs from clinoptilolite on filter paper using 2.0 M HNO_3 and analysis by ICP-OES). These standards were called matrix-matched standards since the resultant solutions were expected to contain very similar matrices as the samples.

Both aqueous and the matrix-matched standard calibration graphs for La, Eu, and Yb are shown in Figures 4.1, 4.2, and 4.3, respectively. Calibration graphs for the remaining REEs are given in Appendix A. As can be seen from these figures, the sensitivity (slope) is affected by sorption/desorption steps and the matrix-matched

standards always gave calibration sensitivities approximately 20 % lower than those of aqueous standards. This is an expected situation when the "% sorption vs. pH and acidity" graphs are examined. As will be shown in the next and the subsequent sections, desorption from the clinoptilolite was achived using 2.0 M HNO_3 solution and even at this HNO_3 concentration, clinoptilolite sorbed approximately 15% of the REEs.

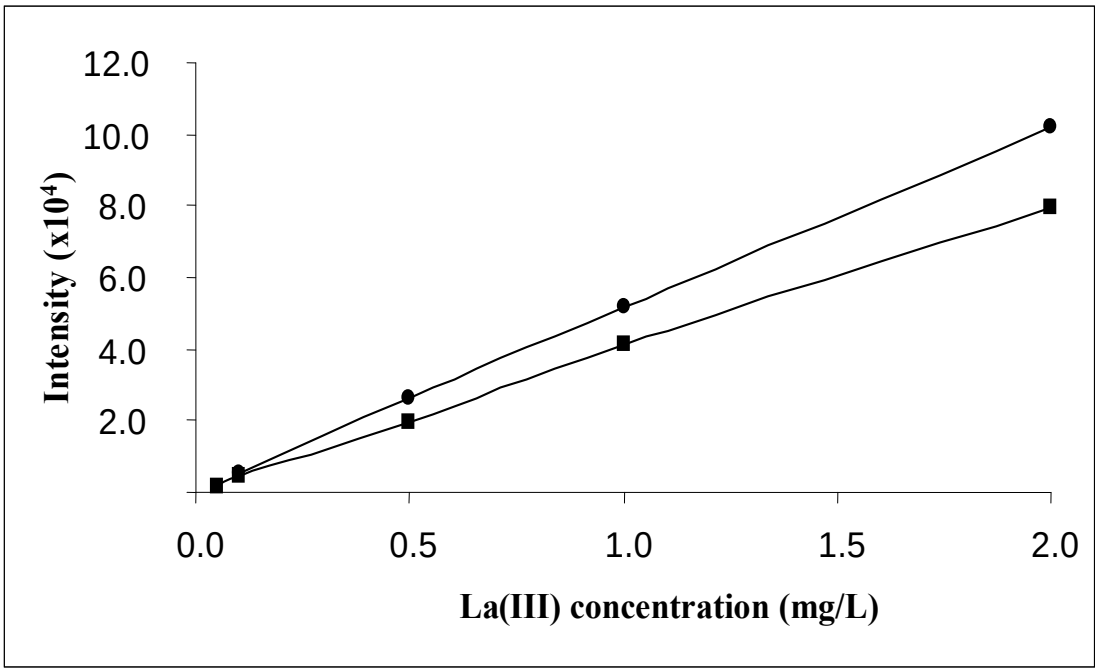

Figure 4.1. Calibration graphs for La(III). (●) La(III) aqueous standard calibration graph (y=50840x + 550.16, R^2=1.0000), (■) La(III) matrix-matched standard calibration graph (y=39948x + 134.93, R^2=0.9996).

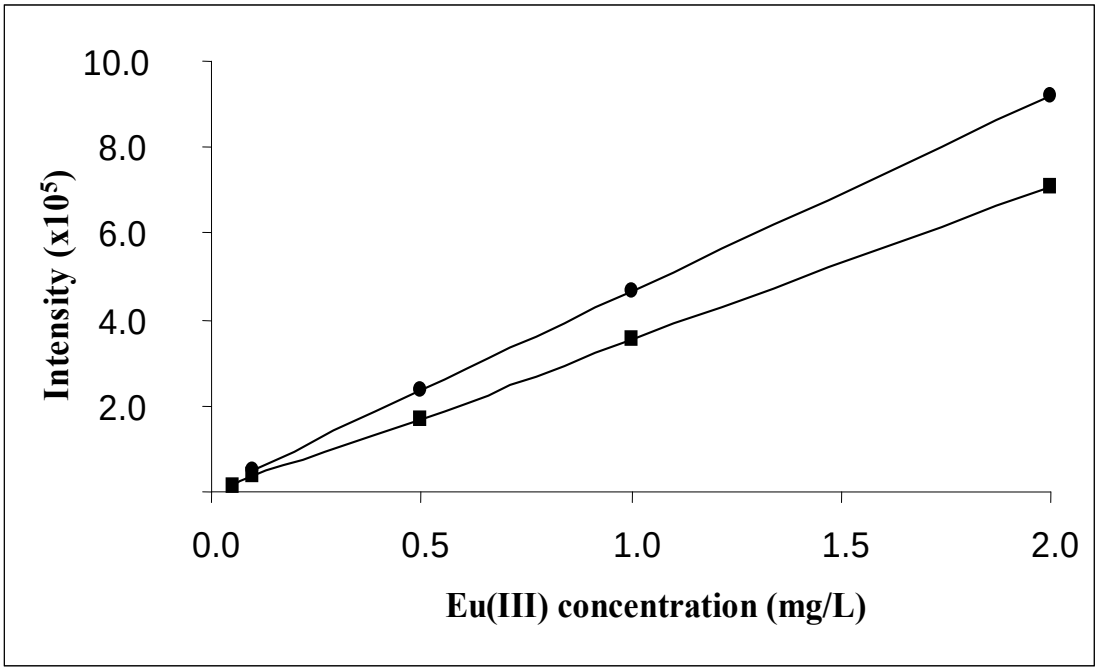

Figure 4.2. Calibration graphs for Eu(III). (●) Eu(III) aqueous standard calibration graph (y=455895x + 6448.3, R^2=1.0000), (■) Eu(III) matrix-matched standard calibration graph (y=355069x + 2913.7, R^2=0.9999).

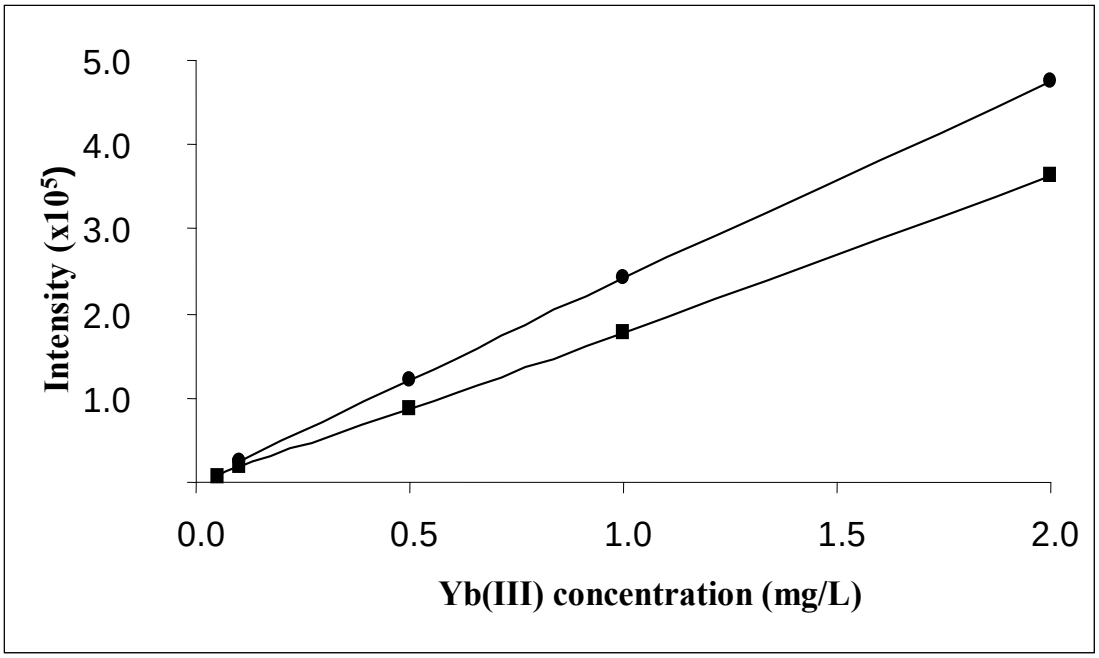

Figure 4.3. Calibration graphs for Yb(III). (●) Yb(III) aqueous standard calibration graph (y=235873x + 3381, R^2=1.0000), (■) Yb(III) matrix-matched standard calibration graph (y=181883x – 2131.8, R^2=0.9998).

4.1.2. Sorption Studies

4.1.2.1. Types of Sorbent

As an initial study, a 1.0 mg/L REEs multi-element standard solution was prepared at a pH of 7 and 20.0 mL aliquots of this solution were mixed with 0.1 g of sorbents as explained in 3.5.2.1. All of the sorbents investigated offered significant results; therefore a detailed study was carried out to understand the effect of pH and acidity on the sorption.

4.1.2.2. Effect of the pH on the Sorption

Effect of pH and acidity was examined as outlined in 3.5.2.2. The percent sorption graphs for La^{+3}, Eu^{+3}, and Yb^{+3} are given in Figures 4.4, 4.5, and 4.6, respectively. Corresponding graphs for the other REEs are given in Appendix B.

As can be seen from the figures, nearly all of the sorbents offer significant results for the sorption of REEs at different pH values. However, especially due to economical reasons it was decided to carry on the further work with clinoptilolite which shows quantitative sorption at pH values greater than 4.0. Clinoptilolite can be found in Turkey naturally in high amounts; therefore, it is the cheapest alternative to the synthetic sorbents.

The acidity part of the figures was very similar for all REEs. Most of the sorbents demonstrated 10-20 % sorption in HNO_3 at concentrations between 0.5 and 4.0M; Amberlite CG-120, Dowex 50W X18, Rexyn 101, and Amberlite IR-120 being exceptions. For these sorbents, the quantitative sorption range extends to 0.5 M HNO_3, which can be very advantageous for the sorption of REEs from acidic samples.

In addition, the low sorption capability (10-15 %) of the sorbent in acidic solutions demonstrated that HNO_3 at these concentrations could be tried as a desorbing solution. This was proven by later experiments and 2.0 M HNO_3 was used as the desorbing solution throughout these studies.

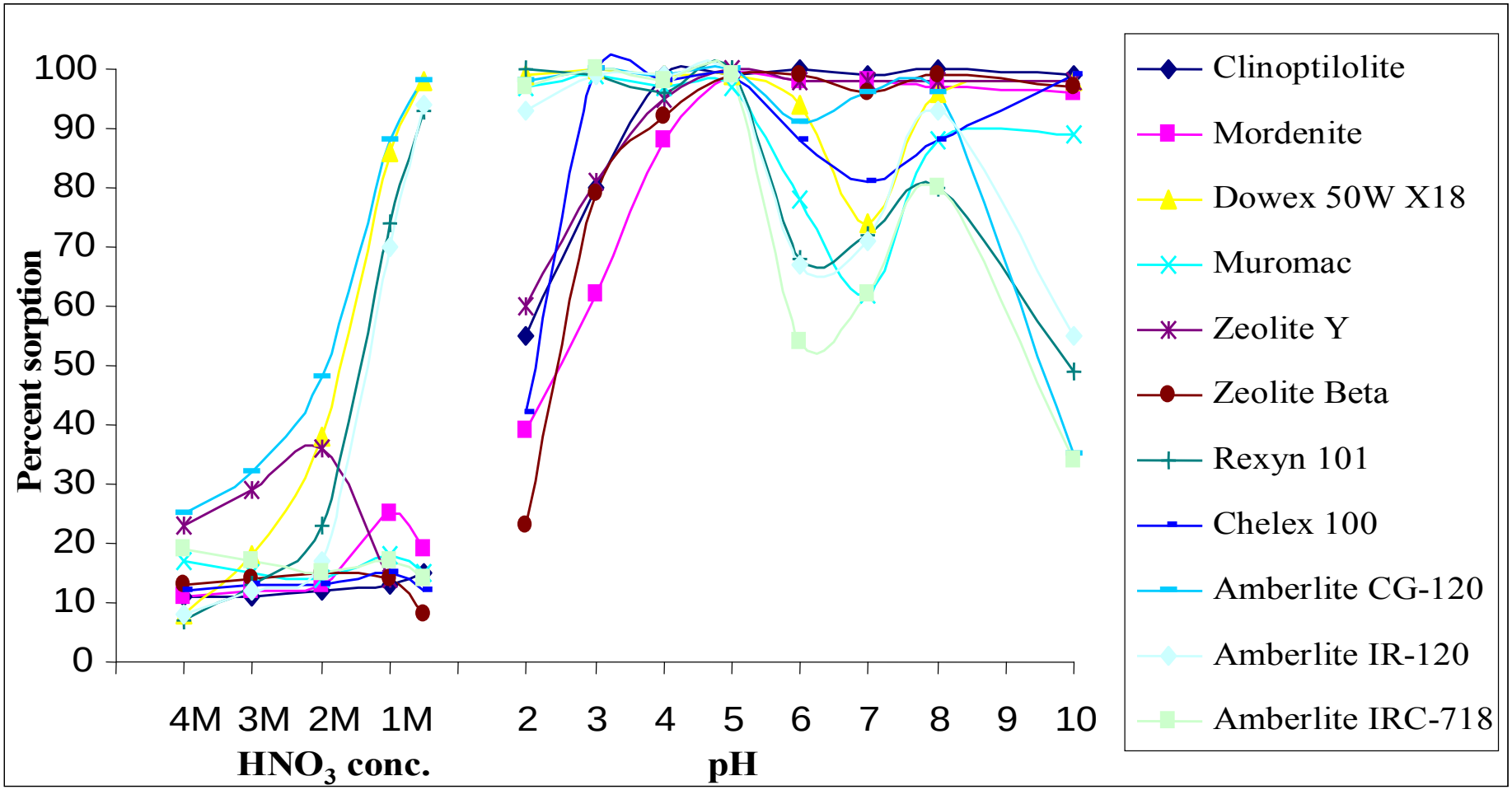

Figure 4.4. Lanthanum sorption as a function of pH and acidity on different sorbents (20.0 mL of 1.0 mg/L solution, sorbent amount: 0.1g)

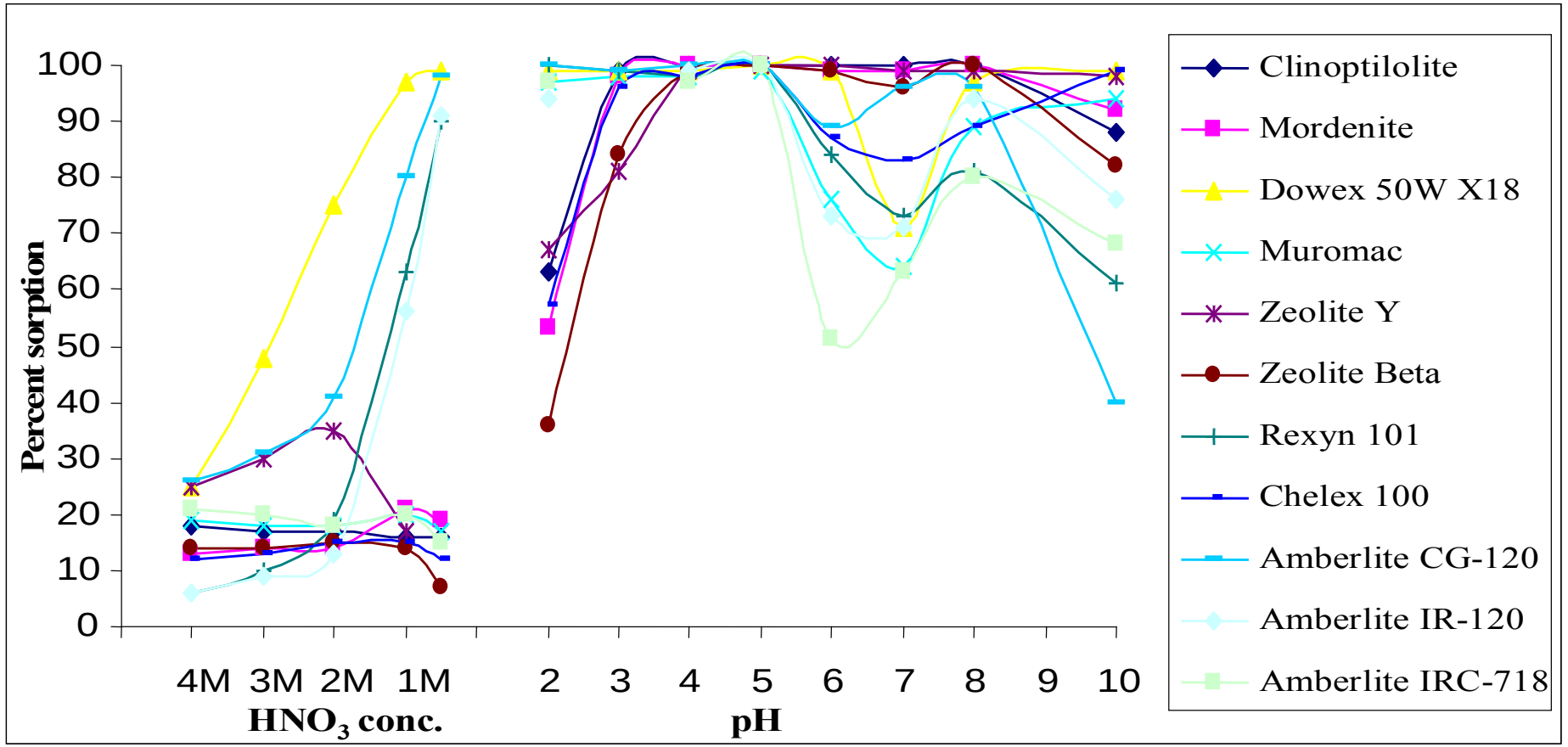

Figure 4.5. Europium sorption as a function of pH and acidity on different sorbents (20.0 mL of 1.0 mg/L solution, sorbent amount: 0.1g)

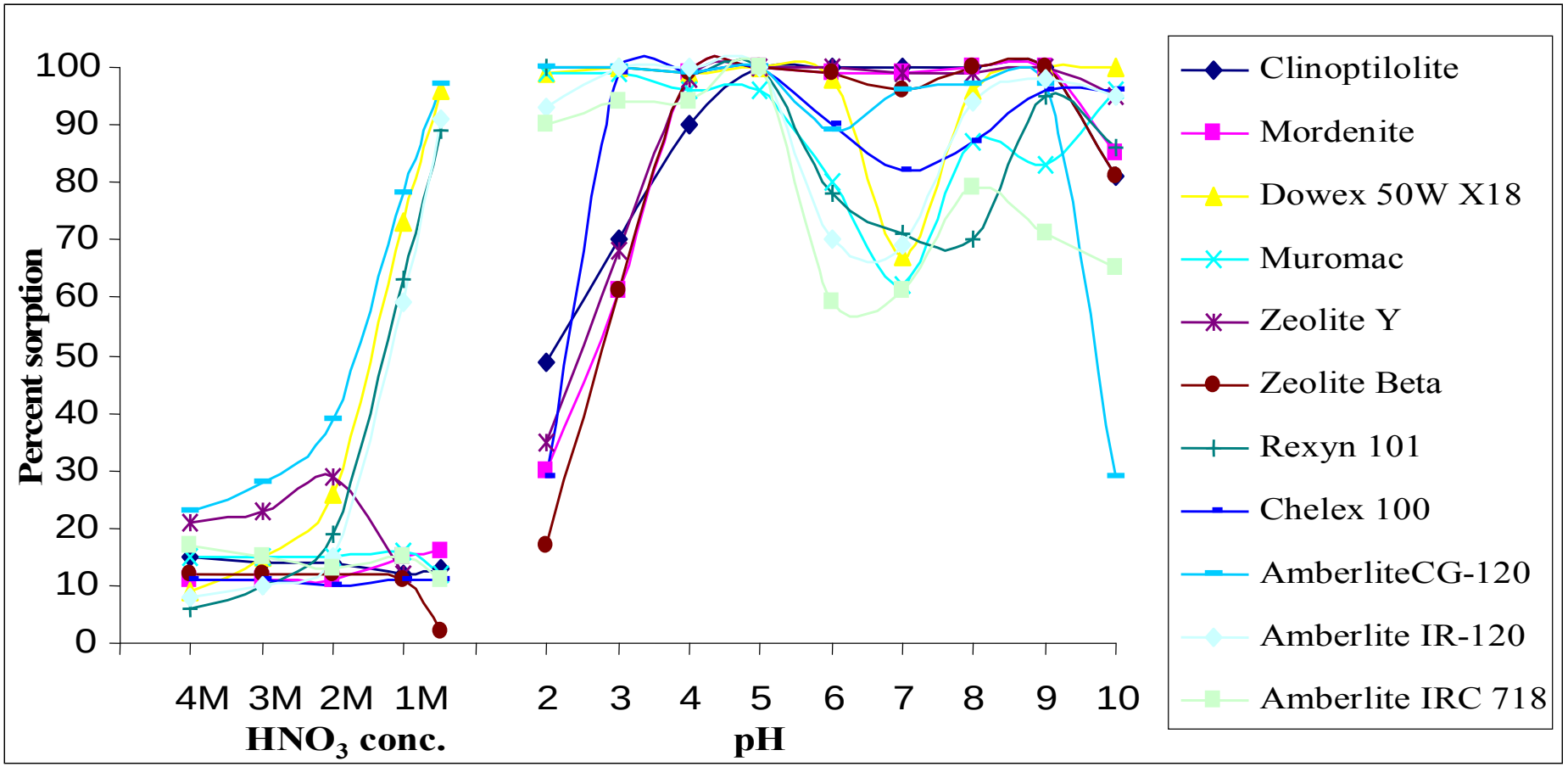

Figure 4.6. Ytterbium sorption as a function of pH and acidity on different sorbents (20.0 mL of 1.0 mg/L solution, sorbent amount: 0.1g)

4.1.2.3. Effect of Shaking Time

Effect of shaking time on the sorption of REEs by clinoptilolite was examined as explained in 3.5.2.3. As can be seen from Figure 4.7, the sorption of REEs by clinoptilolite has very fast kinetic in such a way that it can take up REEs quantitatively from solution even in one minute, at least at the concentration ranges studied (20 mL of 1.0 mg/L). This fast kinetics can also be a good indication of the applicability of the system to column applications. However, a shaking time of 30 minutes was applied in the subsequent experiments.

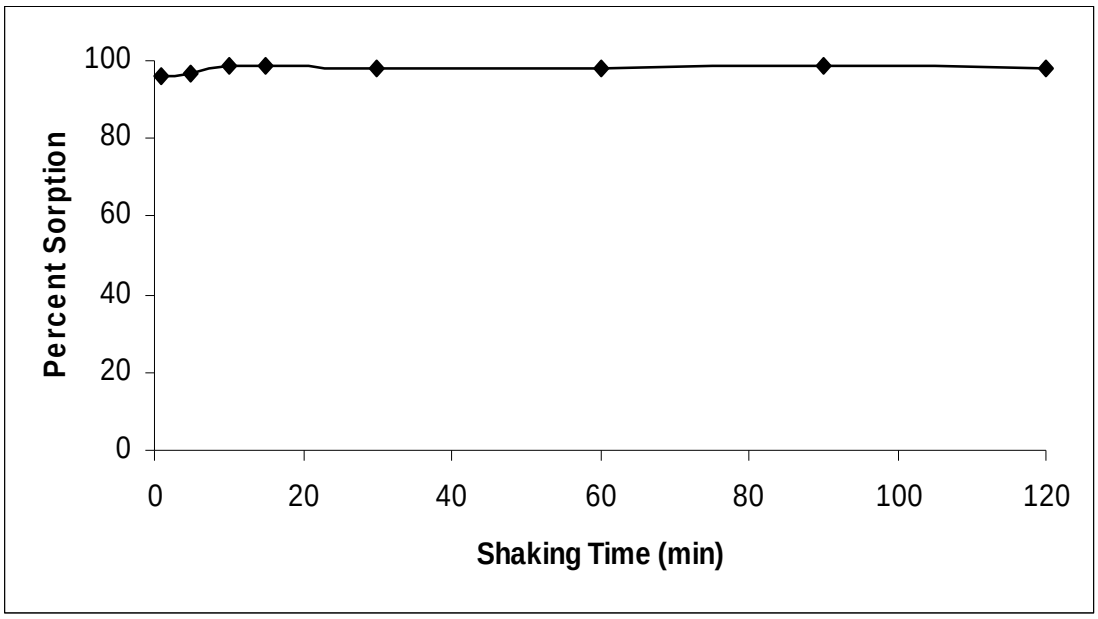

Figure 4.7. Effect of shaking time on sorption of La(III).
(1.0 mg/L La(III), sample volume=20.0 mL, amount of sorbent= 0.1 g, pH=7)

4.1.2.4. Effect of Sorbent Amount

By keeping REEs concentrations constant and increasing the amount of clinoptilolite, sorption of REEs was investigated as explained in section 3.5.2.4. As can be seen from Figure 4.8, even 0.02 g clinoptilolite had a sorption of approximately 95%. In the subsequent experiments, however, 0.1 g of clinoptilolite was used in order to guarantee a more efficient mixing.

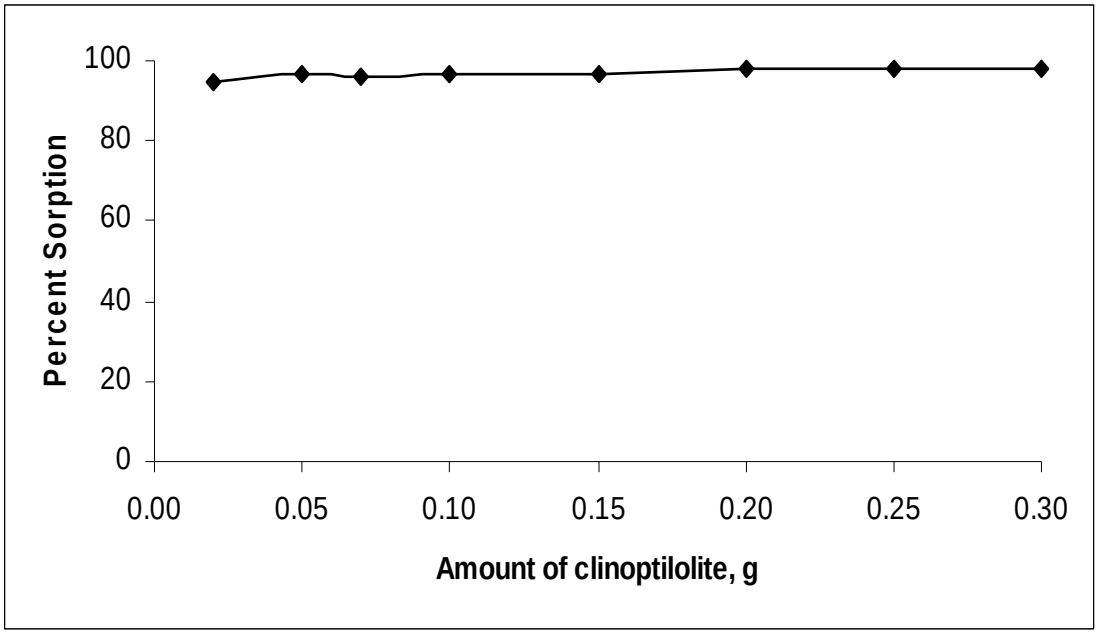

Figure 4.8. Percent sorption of La(III) as a function of clinoptilolite amount (1.0 mg/L La(III), sample volume=20.0 mL, pH=7)

4.1.3. Determination of Sorption Isotherms

To understand the sorption phenomenon of clinoptilolite, sorption isotherms were determined. By doing this we could predict whether the sorption is homogeneous or heterogeneous or takes place in a monolayer or multilayer fashion. In addition, these sorption isotherms can be used for the determination of sorption capacity and are very useful in the prediction of the sorbent amount required for a quantitative sorption.

All sorption experiments were performed in the batch mode. The equilibrium relationship between the adsorbed metal amount per unit mass of clinoptilolite ($[C]_s$) and the residual REEs ion concentration ($[C]_l$) in solution phase was expressed by sorption isotherms. The REEs concentrations were changed from 0.01 to 10.0 mg/L while the amount of the solid in each case was held constant at 0.1 g. The applicability of the Langmuir and Freundlich sorption isotherms was tested under these specified conditions. For Langmuir sorption isotherm, $[C]_s$ versus $[C]_s/[C]_l$ and for the Freundlich sorption isotherm, log $[C]_s$ versus log $[C]_l$ graphs were plotted as shown in Figs. 4.9, 4.10, and 4.11.

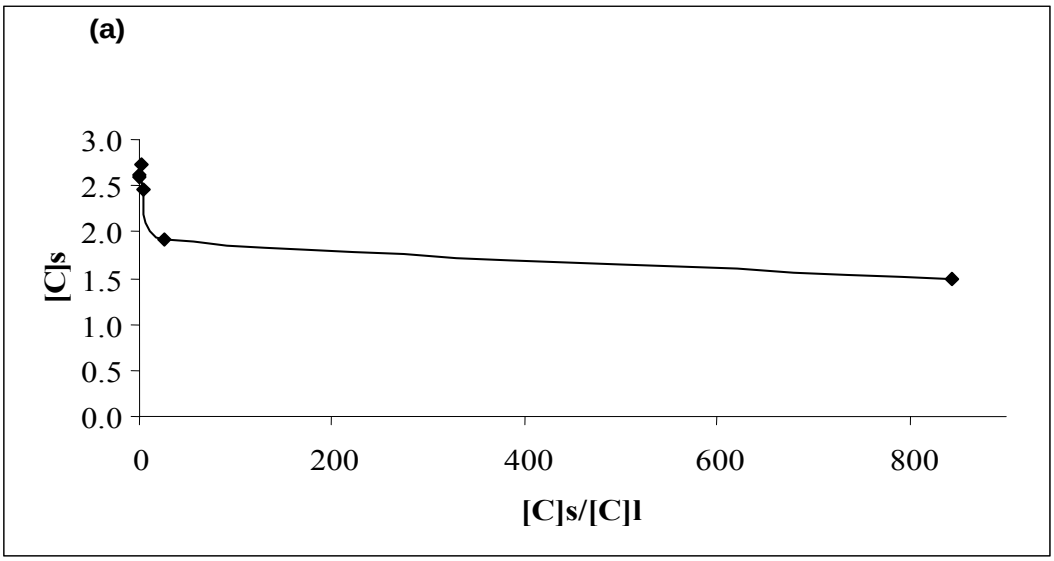

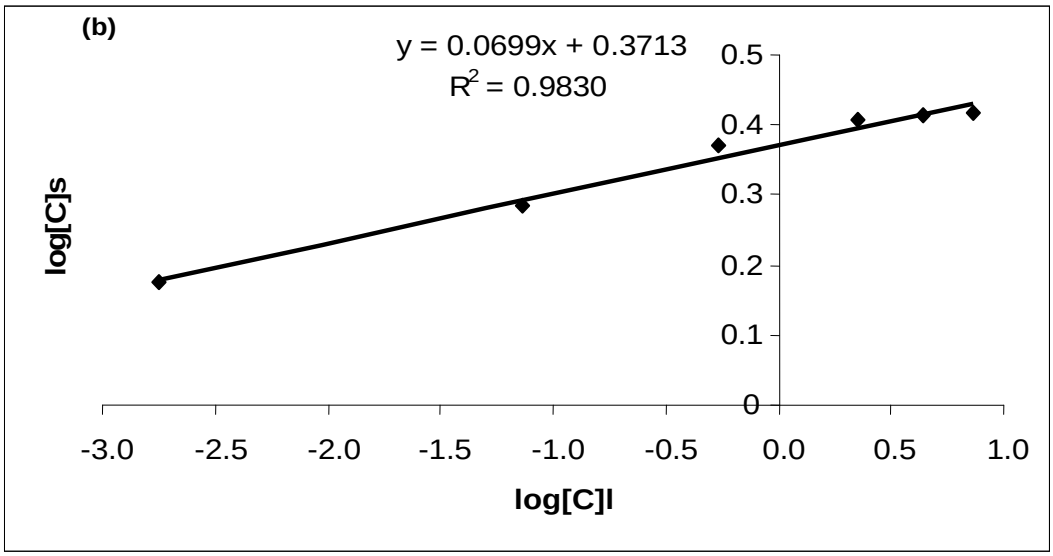

Figure 4.9 (a) Langmuir sorption isotherm for La(III); **(b)** Freundlich sorption isotherm for La(III).

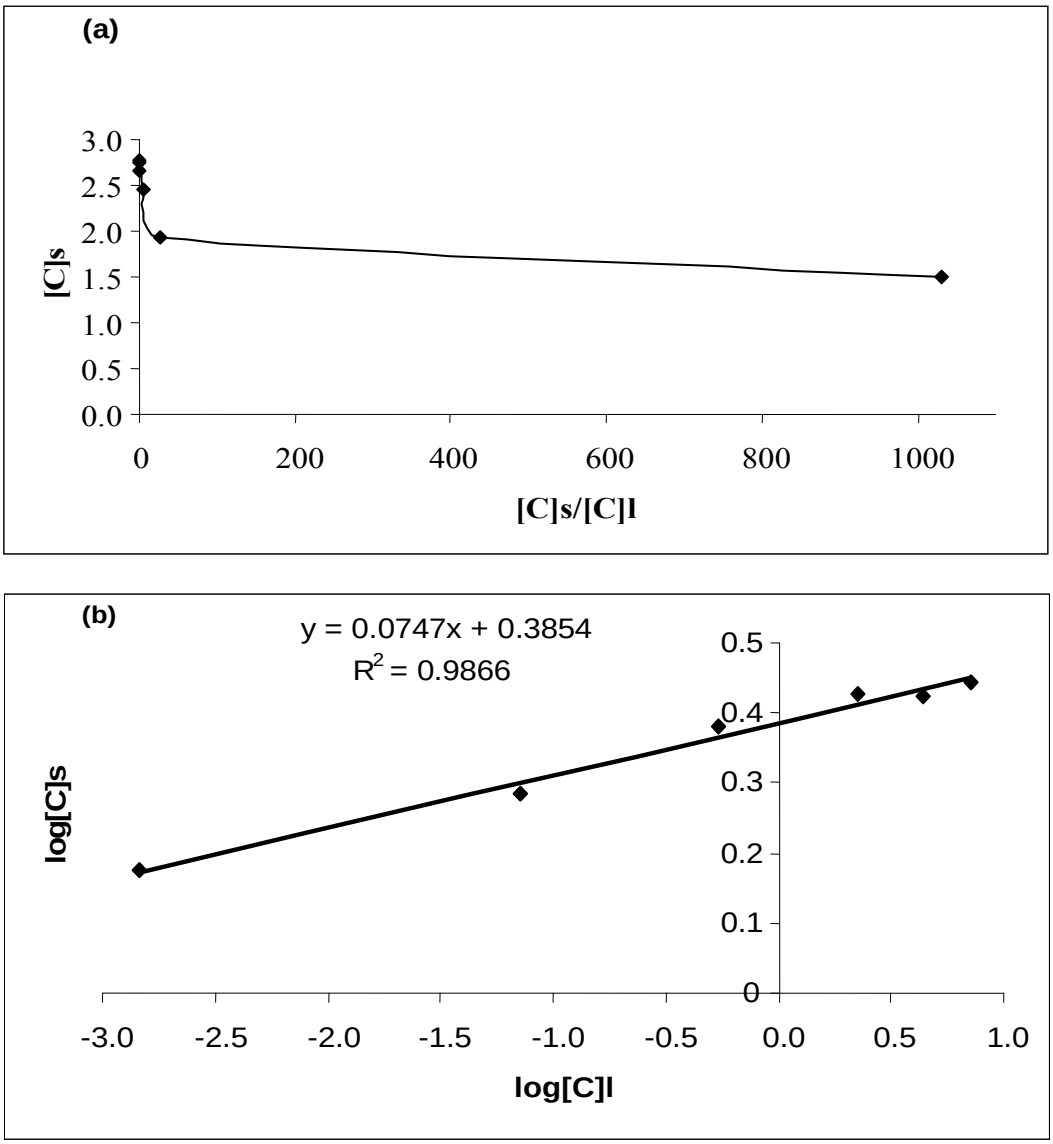

Figure 4.10 (a) Langmuir sorption isotherm for Eu(III); **(b)** Freundlich sorption isotherm for Eu(III).

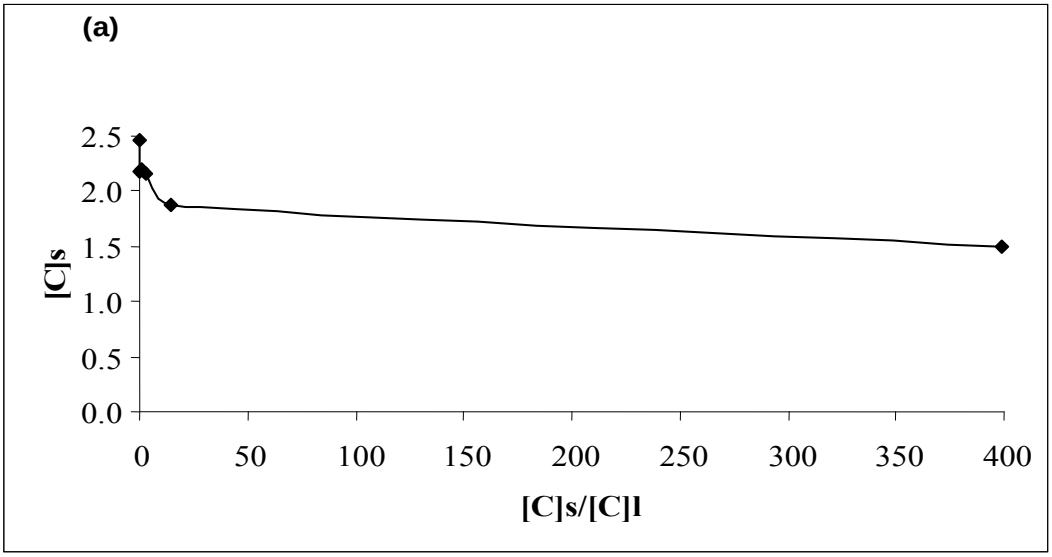

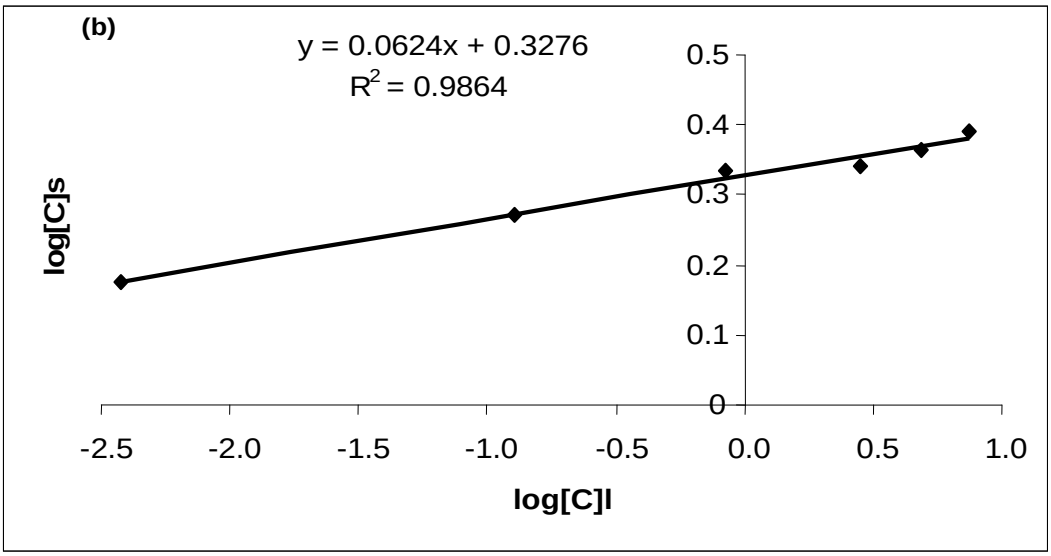

Figure 4.11 (a) Langmuir sorption isotherm for Yb(III); **(b)** Freundlich sorption isotherm for Yb(III).

According to the data obtained, because of having good linearity of sorption it can be said that the Freundlich isotherm is more suitable than the Langmuir isotherm for explaining the sorption behaviour of clinoptilolite. We can predict that clinoptilolite has heterogeneous sorption sites, may exhibit multilayer sorption.

4.1.4. Desorption from Clinoptilolite

Two different strategies were followed for desorption of previously sorbed REEs by clinoptilolite: ion-exchange with Na^+ and K^+, and washing the sorbent with HNO_3 (which can also be considered as ion-exchange, but, with H^+). As an initial experiment, 0.1 M KCl and 0.1 M NaCl were chosen and tried for desorption. As given in Table 4.2, these two solutions at this concentration were not capable of desorbing REEs from clinoptilolite. We did not want to increase the salt concentration since we could have had ionization problems in the ICP.

Another candidate for desorption was HNO_3, since clinoptilolite had a percent sorption value of approximately 15% in 0.5-4.0 M HNO_3 (section 4.1.2.2; Figures 4.4, 4.5, and 4.6). Similarly, upon shaking clinoptilolite with these solutions, the previously-sorbed REEs were eluted from clinoptilolite, and resultant solutions were analyzed by ICP-OES. Elution efficiencies (percent recoveries) were calculated for various concentrations of HNO_3 are given in Table 4.2. These values were between 70-90 % with 2.0 M HNO_3 giving a maximum recovery of 90%. Therefore, 2.0 M HNO_3 was chosen as the desorption solution (eluent) and was used in the subsequent experiments. X-ray diffraction analysis revealed that the treatment of clinoptilolite with 2.0M HNO_3 did not affect the structure of the mineral. The XRPD patterns of natural clinoptilolite and acid treated clinoptilolite are shown in Figure 4.12. The figure indicates that neither the intensity nor the positions of the basic reflections were significantly affected upon treatment with 2.0M HNO_3 acid.

Table 4.1. Desorption of sorbed La(III) from clinoptilolite

Eluent	% Recovery
0.5 M HNO_3	~ 84
1.0 M HNO_3	~ 70
2.0 M HNO_3	~ 90
4.0 M HNO_3	~ 75
0.1 M KCl	~ 2
0.1 M NaCl	~ 10

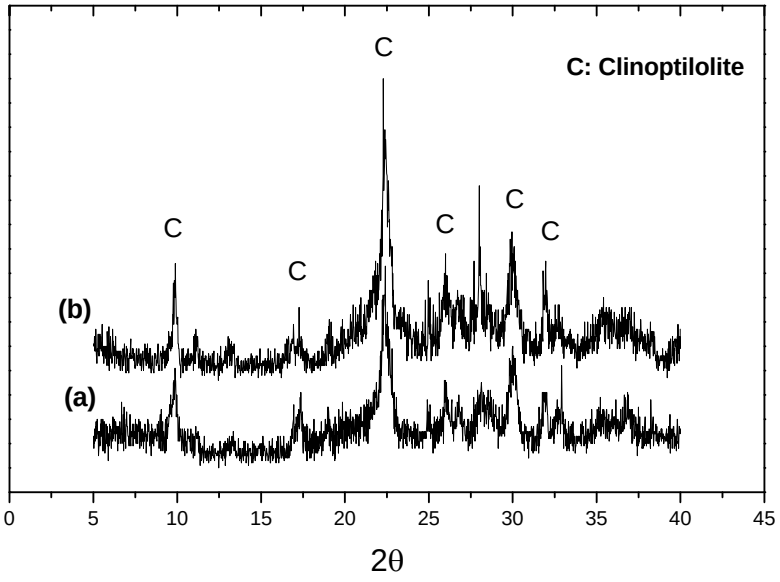

Figure 4.12. (a) XRD pattern of clinoptilolite, **(b)** XRD pattern of acid-treated clinoptilolite with 2M HNO_3

4.1.5. Performance of Preconcentration Steps

In order to investigate the preconcentration efficiency of clinoptilolite with the proposed method, the sorption studies were performed using various volumes from 20-1000 mL of water samples including ultra-pure water, bottled drinking water, river water, sea water and tap water. The final volume of the eluent solution was 20.0 mL. The respective results for the selected REEs (La, Eu, and Yb) are depicted in Tables 4.3 to 4.5 for ultra-pure water, Tables 4.6 to 4.8 for bottled drinking water, Tables 4.9 to 4.11 for river water, Tables 4.12 to 4.14 for sea water, and Tables 4.15 to 4.17 for tap water.

Table 4.2. La(III) recovery results for ultra-pure water (n=5).

La(III) spike (mg/L)	Initial Volume (mL)	Final Volume (mL)	Enrichment Factor	La(III) found (mg/L)	Recovery (%)
0.40	50	20	2.5	0.85 (± 0.02)	85 (± 3)
0.20	100	20	5.0	0.83 (±0.02)	83 (± 2)
0.08	250	20	12.5	0.84 (± 0.03)	84 (± 3)
0.04	500	20	25.0	0.83 (± 0.01)	83 (± 1)
0.02	1000	20	50.0	0.77 (± 0.01)	77 (± 1)

Table 4.3. Eu(III) recovery results for ultra-pure water (n=5).

Eu(III) spike (mg/L)	Initial Volume (mL)	Final Volume (mL)	Enrichment Factor	Eu(III) found (mg/L)	Recovery (%)
0.40	50	20	2.5	0.87 (± 0.01)	87 (± 1)
0.20	100	20	5.0	0.83 (± 0.03)	83 (± 3)
0.08	250	20	12.5	0.82 (± 0.04)	82 (± 4)
0.04	500	20	25.0	0.82 (± 0.02)	82 (± 2)
0.02	1000	20	50.0	0.77 (± 0.77)	77 (± 2)

Table 4.4. Yb(III) recovery results for ultra-pure water (n=5).

Yb(III) spike (mg/L)	Initial Volume (mL)	Final Volume (mL)	Enrichment Factor	Yb(III) found (mg/L)	Recovery (%)
0.40	50	20	2.5	0.92 (± 0.01)	92 (± 1)
0.20	100	20	5.0	0.87 (± 0.03)	87 (± 3)
0.08	250	20	12.5	0.87 (± 0.03)	87 (± 3)
0.04	500	20	25.0	0.87 (± 0.02)	87 (± 2)
0.02	1000	20	50.0	0.79 (± 0.02)	79 (± 2)

Table 4.5. La(III) recovery results for bottled drinking water (n=3).

La(III) spike (mg/L)	Initial Volume (mL)	Final Volume (mL)	Enrichment Factor	La(III) found (mg/L)	Recovery (%)
0.40	50	20	2.5	0.83 (± 0.03)	83 (± 3)
0.20	100	20	5.0	0.84 (± 0.03)	84 (± 3)
0.08	250	20	12.5	0.83 (± 0.04)	83 (± 4)
0.04	500	20	25.0	0.82 (± 0.02)	82 (± 2)
0.02	1000	20	50.0	0.79 (± 0.02)	79 (± 2)

Table 4.6. Eu(III) recovery results for bottled drinking water (n=3).

Eu(III) spike (mg/L)	Initial Volume (mL)	Final Volume (mL)	Enrichment Factor	Eu(III) found (mg/L)	Recovery (%)
0.40	50	20	2.5	0.83 (± 0.03)	83 (± 3)
0.20	100	20	5.0	0.81 (± 0.03)	81 (± 3)
0.08	250	20	12.5	0.81 (± 0.03)	81 (± 3)
0.04	500	20	25.0	0.81 (± 0.03)	81 (± 3)
0.02	1000	20	50.0	0.71 (± 0.02)	71 (± 2)

Table 4.7. Yb(III) recovery results for bottled drinking water (n=3).

Yb(III) spike (mg/L)	Initial Volume (mL)	Final Volume (mL)	Enrichment Factor	Yb(III) found (mg/L)	Recovery (%)
0.40	50	20	2.5	0.87 (± 0.04)	87 (± 4)
0.20	100	20	5.0	0.85 (± 0.03)	85 (± 3)
0.08	250	20	12.5	0.84 (± 0.04)	84 (± 4)
0.04	500	20	25.0	0.86 (± 0.02)	86 (± 2)
0.02	1000	20	50.0	0.83 (± 0.00)	83 (± 1)

Table 4.8. La(III) recovery results for river water (n=3).

La(III) spike (mg/L)	Initial Volume (mL)	Final Volume (mL)	Enrichment Factor	La(III) found (mg/L)	Recovery (%)
0.40	50	20	2.5	0.84 (± 0.02)	84 (± 2)
0.20	100	20	5.0	0.79 (± 0.04)	79 (± 4)
0.08	250	20	12.5	0.65 (± 0.03)	65 (± 3)
0.04	500	20	25.0	0.66 (± 0.02)	66 (± 2)
0.02	1000	20	50.0	0.65 (± 0.03)	65 (± 3)

Table 4.9. Eu(III) recovery results for river water (n=3).

Eu(III) spike (mg/L)	Initial Volume (mL)	Final Volume (mL)	Enrichment Factor	Eu(III) found (mg/L)	Recovery (%)
0.40	50	20	2.5	0.81 (± 0.01)	81 (± 1)
0.20	100	20	5.0	0.76 (± 0.01)	76 (± 1)
0.08	250	20	12.5	0.63 (± 0.01)	63 (± 1)
0.04	500	20	25.0	0.63 (± 0.01)	64 (± 1)
0.02	1000	20	50.0	0.64 (± 0.02)	64 (± 2)

Table 4.10. Yb(III) recovery results for river water (n=3).

Yb(III) spike (mg/L)	Initial Volume (mL)	Final Volume (mL)	Enrichment Factor	Yb(III) found (mg/L)	Recovery (%)
0.40	50	20	2.5	0.82 (± 0.02)	82 (± 2)
0.20	100	20	5.0	0.76 (± 0.02)	76 (± 2)
0.08	250	20	12.5	0.65 (± 0.03)	65 (± 3)
0.04	500	20	25.0	0.65 (± 0.02)	65 (± 2)
0.02	1000	20	50.0	0.64 (± 0.03)	64 (± 3)

Table 4.11. La(III) recovery results for sea water (n=3).

Eu(III) spike (mg/L)	Initial Volume (mL)	Final Volume (mL)	Enrichment Factor	Eu(III) found (mg/L)	Recovery (%)
0.40	50	20	2.5	0.83 (± 0.03)	83 (± 3)
0.20	100	20	5.0	0.75 (± 0.01)	75 (± 1)
0.08	250	20	12.5	0.61 (± 0.01)	61 (± 1)
0.04	500	20	25.0	0.53 (± 0.01)	53 (± 1)
0.02	1000	20	50.0	0.48 (± 0.01)	48 (± 1)

Table 4.12. Eu(III) recovery results for sea water (n=3).

Eu(III) spike (mg/L)	Initial Volume (mL)	Final Volume (mL)	Enrichment Factor	Eu(III) found (mg/L)	Recovery (%)
0.40	50	20	2.5	0.84 (± 0.02)	84 (± 2)
0.20	100	20	5.0	0.74 (± 0.01)	74 (± 1)
0.08	250	20	12.5	0.61 (± 0.02)	61 (± 2)
0.04	500	20	25.0	0.53 (± 0.02)	53 (± 2)
0.02	1000	20	50.0	0.42 (± 0.01)	42 (± 1)

Table 4.13. Yb(III) recovery results for sea water (n=3).

Yb(III) spike (mg/L)	Initial Volume (mL)	Final Volume (mL)	Enrichment Factor	Yb(III) found (mg/L)	Recovery (%)
0.40	50	20	2.5	0.85 (± 0.03)	85 (± 3)
0.20	100	20	5.0	0.77 (± 0.01)	77 (± 1)
0.08	250	20	12.5	0.67 (± 0.02)	67 (± 2)
0.04	500	20	25.0	0.56 (± 0.03)	56 (± 3)
0.02	1000	20	50.0	0.52 (± 0.03)	52 (± 3)

Table 4.14. La(III) recovery results for tap water (n=3).

La(III) spike (mg/L)	Initial Volume (mL)	Final Volume (mL)	Enrichment Factor	La(III) found (mg/L)	Recovery (%)
0.40	50	20	2.5	0.87 (± 0.01)	87 (± 1)
0.20	100	20	5.0	0.82 (± 0.01)	82 (± 1)
0.08	250	20	12.5	0.63 (± 0.02)	63 (± 2)
0.04	500	20	25.0	0.46 (± 0.01)	46 (± 1)
0.02	1000	20	50.0	0.36 (± 0.02)	36 (± 2)

Table 4.15. Eu(III) recovery results for tap water (n=3)

Eu(III) spike (mg/L)	Initial Volume (mL)	Final Volume (mL)	Enrichment Factor	Eu(III) found (mg/L)	Recovery (%)
0.40	50	20	2.5	0.86 (± 0.02)	86(± 2)
0.20	100	20	5.0	0.81 (± 0.01)	81(± 1)
0.08	250	20	12.5	0.62 (± 0.01)	62 (± 1)
0.04	500	20	25.0	0.52 (± 0.03)	52 (± 3)
0.02	1000	20	50.0	0.39 (± 0.03)	39 (± 3)

Table 4.16. Yb(III) recovery results for tap water (n=3).

Yb(III) spike (mg/L)	Initial Volume (mL)	Final Volume (mL)	Enrichment Factor	Yb(III) found (mg/L)	Recovery (%)
0.40	50	20	2.5	0.84 (± 0.01)	84 (± 1)
0.20	100	20	5.0	0.74 (± 0.03)	74 (± 3)
0.08	250	20	12.5	0.59 (± 0.02)	59 (± 2)
0.04	500	20	25.0	0.56 (± 0.01)	56 (± 1)
0.02	1000	20	50.0	0.47 (± 0.01)	47 (± 1)

As can be seen from Tables 4.2 to 4.4, the proposed methodology with clinoptilolite works efficiently in ultra-pure water for separation and/or preconcentration purposes for all REEs (only three of them are given here). A similar behavior was observed for bottled drinking water for all the initial volumes (Tables 4.5 to 4.7). The relatively simple matrices of ultra-pure and bottled drinking waters enable high preconcentration factors to be attained in addition to the capability of the method for separation. For example, even for an initial volume of 1000 mL for these two types of water samples (a preconcentration factor of 50 when final volume was 20 mL), the total recovery decreased only about 5 to 10 percent.

The method was very efficient for river water too, especially for the initial volumes of 50 and 100 mL (Tables 4.8 to 4.10). But when the initial volume increased beyond 250 mL, the recoveries were lowered to about 65 percent. This average recovery value can be considered being sufficient for many studies containing similar matrices.

For the remaining two types of waters, namely sea water and tap water, the total recoveries were acceptable for the first two initial volumes (50 mL and 100 mL) and changed from 85 to 75 percent, respectively. As can be seen from Tables 4.11 to 4.13 (for sea water), and from Tables 4.14 to 4.16 (for tap water), the method can still be applied for the initial volume of 250 mL with a total recovery of 60 percent whereas for higher volumes (500 mL and 1000 mL) the recoveries decrease to below 60 percent. These lower recoveries were expected for sea water samples for high volumes since it is known to have a very difficult matrix. But the lower recoveries obtained with higher volume of tap water were quite interesting in such a way that a similar behavior was observed for antimony determination that had been carried out by our group (Erdem 2003). This effect can be referred to the very hard nature of tap water of Urla Municipality.

Due to the absence of a standard reference material containing similar matrices and proper concentrations of REEs, the method validation was realized through the above-mentioned spike recovery tests. As discussed in the preceding paragraphs, these recovery values might demonstrate the efficiency of the proposed methodology.

CONCLUSION

Determination of rare earth elements in environmental samples is usually performed by plasma techniques such as ICP-OES and ICP-MS. Although these techniques enable very sensitive determinations for REEs, it may still be necessary to apply a preconcentration step due to their low concentrations in certain samples. In addition, the presence of heavy matrix in some matrices may necessitate an efficient separation/matrix removal step to be employed prior to instrumental measurements.

In this thesis, a new method was proposed for the separation and/or preconcentration of REEs in environmental samples prior to their determination by ICP-OES. For this purpose different types of zeolites (clinoptilolite, mordenite, zeolite Y, zeolite Beta), ion exchangers (Amberlite CG-120, Amberlite IR-120, Rexyn 101, Dowex 50W X18) and chelating resins (Muromac, Chelex 100, Amberlite IRC-718) were tested as adsorbent materials. Initial studies were concentrated on the investigation of a proper adsorbent for the sorption of REEs. Most of the tested adsorbents demonstrated an efficient sorption capability in a broad pH range. The choice of the adsorbent will be based on the working pH; some of them being applicable even at very low pHs. Considering the natural pH range of many of the environmental samples and also due to the economical reasons, clinoptilolite, a natural and very abundant zeolite in Turkey, was decided to be the most appropriate sorbent for this study. It has shown very fast kinetics during sorption in such a way that it can take up REEs quantitatively from solution even in one minute, at least at the concentration ranges studied (20 mL of 1 mg/L). This fast kinetics can also be a good indication of the applicability of the system to column applications. By the way, we have not tried any column filled with clinoptilolite due to its small particle size (<38 μm) which could have created a back-pressure during flow. The use of mini- or micro-columns can also be very advantageous during enrichment step and can allow higher preconcentration factors to be attained since the elution can be realized with only a few milliliters of the eluent even if relatively higher sample volumes (>100 mL) are processed. In the present system, the eluent volume is 20 mL.

It should also be mentioned here that the proposed methodology can be coupled to other detection systems in addition to ICP-OES. For example ICP-MS, with its very

fast and superior detection capability, can be a more efficient alternative to ICP-OES, especially when used together with microcolumns.

The applicability of the method to real samples was examined by spike recovery tests. The percent recoveries for ultra pure water, bottled drinking water, and river water were sufficient at different initial volumes. But, due to the presence of matrix effects, percent recoveries of REEs from sea water and tap water were low when the initial volumes were higher than 100 mL. In all quantification processes including spike recovery studies, two strategies were followed in drawing the calibration graphs. First, a plot was obtained with aqueous calibration standards, and the other graph with matrix-matched standards. The matrix-matched standard graph was obtained by applying the proposed sorption/desorption steps with clinoptilolite. Matrix-matching was applied even with spiked ultra pure water, the reason being not the suppression effect of the sample pretreated but the matrix of the eluate that originates from clinoptilolite (after sorption, clinoptilolite was being shaken with 2.0 M HNO_3, possibly eluting other ions from the material).

REFERENCES

Ackley A., Yang R. T., "Diffusion in Ion Exchanged Clinoptilolites", *AIChE Journal*, **37(11)**, (1991a), 1645-1656.

Ackley M., Giese R. F., Yand R. T., "Clinoptilolite: Untapped Potential for Kinetic Gas Separations", Zeolites, **12** (September/October), (1992), 780-788.

Allen E. R., Ming D. W., "Recent Progress in the Use of Natural Zeolites in Agronomy and Horticulture", *International Committee on Natural Zeolites,* New York, (1995), 477-490.

Arcoya A., Gonzales J. A., Travieso N., Seoane X. L., "Physicochemical and Catalytic Properties of a Modified Natural Clinoptilolite", *Clays and Clay Minerals*, **29**, (1994,9, 123-131.

Breck D. W., "Zeolite Molecular Sieves Structure, Chemistry and Use", *Wiley Interscience*, New York, (1974).

Brzyska W., "Lanthanides and Actinides", Wydawnictwa Naukowo-Techniczne Poland, (1996), 40-41.

Crock J. G. and Lichte F. E., "Determination of rare earth elements in geological materials by inductively coupled argon plasma/atomic emission spectrometry", *Anal. Chem.*, **54**, (1982), 1329.

Crock J. G., Lichte F. E., Riddle G. O. and. Beech C. L**, "**Separation and preconcentration of the rare-earth elements and yttrium from geological materials by ion-exchange and sequential acid elution", *Talanta*, **33**, (1986), 601.

Dev Kapil, Rita Pathak and Rao G. N.*, "*Sorption behaviour of lanthanum(III), neodymium(III), terbium(III), thorium(IV) and uranium(VI) on Amberlite XAD-4 resin functionalized with bicine ligands", *Talanta,* **48***,* (1999), 579.

De Baar Hein J. W., Michael P.Bacon and Peter G. Brewer Kenneth W. Bruland, "Rare earth elements in the Pacific and Atlantic Oceans", *Geochim Comsochim Acta.,* **49**, (1985), 1943.

Djingova R., Ivonova J., "Determination of rare earth elements in soils and sediments by inductively coupled plasma atomic emission spectrometry after cation-Exchange separation", *Talanta*, **57***,* Issue 5, (2002), 821-829.

Eberl D. D., Barbarick K. A., Lai T. M., Influence of NH4-Exchanged Clinoptilolite on Nutrient Concentrations in Sorgham-Sudangrass", *International Committee on Natural Zeolites,* New York, (1995), 491-513.

Erdem Asli, "Speciation and Preconcentration of Inorganic Antimony and Manganese in Waters Using Mirocolumn-Flow Injection system and Determination by Atomic Absorption Spectrometry", Master of Science Thesis in Chemistry IYTE, (2003).

Evans C.H., "Episodes from the History of the Rare Earth Elements", University of Pittsburgh*, PA, USA*, **15**, (1997).

Figueiredo A.M.G., Avristcher W., Masini E.A., Diniz S.C, Abrao A., "Determination of lanthanides (La, Ce, Nd, Sm) and other elements in metallic gallium by instrumental neutron activation analysis", *Journal of Alloys and Compounds,* **344**, (2002), 36–39.

Gottardi G., Galli E., "Natural Zeolites", *Springer-Verlag*, Berlin, (1985).

Greaves M. J., Elderfield H. and Klinkhammer G. P., "Determination of the rare earth elements in natural waters by isotope-dilution mass spectrometry", *Anal. Chim. Acta.,* **218**, (1989), 265.

Grebneva O. N., Kuzmin N. M., Tsysin G. I. and Zolotov Yu. A., "On-line-sorption preconcentration and inductively coupled plasma atomic emission spectrometry determination of rare earth elements", *Spectrochim Acta,* **51B**, (1996), 1417.

Gorbunov A.V.,. Frontasyeva M.V, Gundorina S.F., Onischenko T.L., Maksuta V.V., Chen Sen Pal., "Evaluation of the effect of agricultural melioration with the use of phosphogypsum on trace element content in soils and vegetation", *Sci. Total Environ.*, **122**, (1992), 337.

Haskin, L.A., Paster, T.P., "Geochemistry and mineralogy of the rare earths." In: Gschneidner Jr, K.A., Eyring, L. (Eds.), *Handbook on the Physics and Chemistry of Rare Earths*, vol. 3. North-Holland, New York, (1979), 1-80.

Henderson, P., "Rare Earth Element Geochemistry." *Elsevier*, New York, (1984).

Hirata Shizuko, Kajiya Tasuku, Aihara Masato, Honda Kazuto, Shikino Osamu, "Determination of rare earth elements in seawater by on-line column preconcentration inductively coupled plasma mass spectrometry", *Talanta*, **58**, (2002), 1185- 1194.

Hoyle J., Elderfield H., "The behaviour of the rare earth elements in the water of luce", *Marine Chemistry*, **12**, (1983), 239.

Iwasaki Kiyoshi, Fuwa Keiichiro and Haraguchi Hiroki,"Simultaneous determination of 14 lanthanides and yttrium in rare earth ores by inductively-coupled plasma atomic emission spectrometry", *Anal. Chim. Acta.,* **183**, (1986), 239-249.

Kawabata K., Kishi Y., Kawaguchi O., Watanabe Y., and Inoue Y., "Determination of rare-earth elements by inductively coupled plasma mass spectrometry with ion chromatography", *Anal. Chem.*, **63**, (1991), 2137.

Kesraoui-Ouki S., Cheeseman C. R., Perry R., "Effects of Conditioning and Treatment of Chabazite and Clinoptilolite Prior to Lead and Cadmium Removal", *Environmental Science and Technology*, **27**, (1993), 1108-1116.

Langade A. D. and Shinde V. M., "Solvent extraction of scandium(III)", *Anal. Chem*., **52**, (1980), 2031.

Liang Lian, D'Haese Patrick C., Lamberts Ludwig V., Van de Vyver Frank L., and De Broe Marc E., "Determination of gadolinium in biological materials using graphite furnace atomic absorption spectrometry with a tantalum boat after solvent extraction", *Anal.Chem*., **63**, (1991), 423.

Liang Pei, Hu Bin, Jiang Zucheng, Qin Yongchao and Peng Tianyou, "Nanometer-sized titanium dioxide micro-column on-line preconcentration of La, Y, Yb, Eu, Dy and their determination by inductively coupled plasma atomic emission spectrometry*", J. Anal. At. Spectrom.*, **16**, (2001), 863.

McLennan S.M., "Rare earth elements in sedimentaryrocks; influence of provenance and sedimentary processes." In: Lipin, B.R., McKay, G.A. (Eds.), *Geochemistry and Mineralogy of Rare Earth Elements*, Mineral Soc. Am. Rev. Min., **21**, (1989), 169-200.

Minowa H., Ebihara M., "Separation of rare earth elements from scandium by extraction chromatography: Application to radiochemical neutron activation analysis for trace rare earth elements in geological samples", *Analytica Chimica Acta*, **498**, (2003), 25–37.

Moscou L., "The Zeolite Scene", "Introduction to Zeolite Science and Practice", van Bekkum H., Flenigen E. M., Jansen J. C., *Elsevier*, Amsterdam, (1991), 1-11.

Möller Peter, Dulski Peter and Luck Joachim, "Determination of rare earth elements in seawater by inductively coupled plasma-mass spectrometry", *Spectrochimica Acta Part B*, **47**, (1992), 1379-1387.

Navarro M.S., Ulbrich H.H.G.J., Andrade S., Janasi V.A., "Adaptation of ICP–OES routine determination techniques for the analysis of rare earth elements by chromatographic separation in geologic materials: tests with reference materials and granitic rocks", *Journal of Alloys and Compounds*, **344**, (2002), 40–45.

Noemia M. P. and Iyer S. S., "Determination of rare earth elements in USGS rock standards by isotope dilution mass spectrometry and comparison with neutron activation and inductively coupled plasma atomic emission spectrometry", *Analytica Chimica Acta, **236*** , (1990), 487-493.

Orvini E., Spezialib M., Salvinic A., Herborga C., "Rare earth elements determination in environmental matrices by INAA", *Microchemical Journal*, **67**, (2000), 97-104.

Palasz Artur, Czekaj Piotr, "Toxicological and cytophysiological aspects of lanthanides action", *II Department of Histology and Embryology,* Silesian Medical Academy, Katowice, Poland, (2000).

Pedreira W.R., Sarkis J.E.S., Rodriguez C., Tomiyoshi I.A.,. da Silva Queiroz C.A, Abrao A., "Determination of trace rare earth elements in high pure lanthanum oxide by sector field inductively coupled plasma mass spectrometry (HR ICP-MS) and high-performance liquid chromatography (HPLC) techniques", *Journal of Alloys and Compounds*, **1**, (2002), 304.

Pond W. G., "Zeolites in Animal Nutrition and Health: A review", *International Committee on Natural Zeolites,* New York, (1995), 449-457.

Qin Shuai, Bin Hu, Yongchao Qin, Ruth Wanjau and Jiang Zucheng, "Determination of trace rare earth impurities in high-purity cerium oxide by using electrothermal vaporization ICP-AES after HPLC separation with 2-ethylhexylhydrogen 2-ethylhexylphosphonate resin as the stationary phase", *J. Anal. At. Spectrom.*, **15**, (2000), 1413 – 1416.

Roychowdhury P., Roy N. K., Das D. K. and Das A. K., "Determination of rare-earth . elements and yttrium in silicate rocks by sequential inductively-coupled plasma . emission spectrometry", *Talanta*, **36**, (1989), 1183.

Rucandio M. I., "Determination of lanthanides and yttrium in rare earth ores and concentrates by inductively coupled plasma atomic emission spectrometry", *Anal. Chim. Acta.*, **264**, (1992), 333-344.

Sabbioni E., Pietra R. and Gaglione P. Vocaturo G, Colombo F., Zanoni M. and Rodi F., "Long-term occupational risk of rare-earth pneumoconiosis A case report as investigated by neutron activation analysis "**,** *Sci. Total. Environ.,* **26***,* (1982), 19-32.

Sax N. I., "Dangerous Properties of Industrial Material", *Van Nostrand Reinhold*, New York, (1984), 2358-2368.

Settle Frank, "Handbook of Instrumental Techniques for Analytical Chemistry", New Jersey, (1997), 395-410.

Shahwan T., "Radiochemical and Spectroscopic Studies of Cesium, Barium, and Cobalt Sorption on Some Natural Clays", *Ph. D. Thesis*, Bilkent University, (2000).

Shuai Qin, Qin Yongchao, Xiong Bin Hu, Houngchun, and Jiang Zucheng, "Determination of rare earth impurities in high-purity lanthanum oxide using electrothermal vaporization/ICP-AES after HPLC Separation", *Anal. Sci.*, **16**, (2000), 957.

Sloof W., Bout P.F., Hoop van den M.A.G.T., Jannus J.A., Annenis J.A., "Exploratory report rare earth metals and their compounds", *National Institute Public Healty and Environmental Protection*, Bilthoven, Netherlands, rep. N 710401025, (1993), 50.

Symth J. R., Spaid A. T., Bish D. L., "Crystal Structures of a Natural and Cs-Exchanged Clinoptilolite", *American Mineralogist*, **75**, (1995), 522-528.

Tsitsishvili G. V., Andronikashvili T. G., Kirov G. N., Filizova L. D., "Natural Zeolites", *Ellis Horwood*, New York, (1992).

Vicente O., Martinez A. Padró, L., Olsina R. and Marchevsky E., "Determination of some rare earth elements in seawater by inductively coupled plasma mass spectrometry using flow injection preconcentration", *Spectrochim Acta,* **53B**, (1998), 1281.

Zachmann D. W., "Matrix effects in the separation of rare earth elements, scandium, and yttrium and their determination by inductively coupled plasma optical emission spectrometry", *Anal. Chem*., **60**, (1988), 420.

Zhao D., Cleare K., Oliver C., Ingram C., Cook D., Szostak R., Kevan L., "Characteristics of the Synthetic Heulandite-Clinoptilolite Family of Zeolites", *Microprous and Mesoporous Materials*, **21**, (1998), 371-379.

Zhu W., de Leer E.W.B, Kennedy M., Alaerts G.J.F.R., " Study of the preconcentration and determination of ultratrace rare earth elements in environmental samples with an ion exchange micro-column", *Fresenius J. Anal Chem*., **360**, (1998), 74-80.

Wang Y.G., Xiong Y., Meng S.L., Li D.Q., " Separation of yttrium from heavy lanthanide by CA-100 using the complexing agent", *Talanta*, **63**, (2004), 239–243.

Wilson, M.,"Igneous Petrogenesis", *A Global Tectonic Approach.*, Chapman&Hall, London, (1989).

APPENDIX A
Aqueous and Matrix-matched Standard Calibration Graphs for REEs

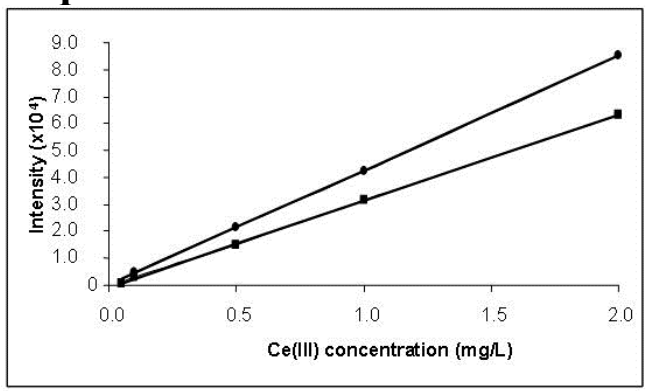

Figure A.1. Calibration graphs for Ce(III). (•) Ce(III) aqueous standard calibration graph (y = 42351x + 288.66, R2 = 1.0000), (■) Ce(III) matrix-matched standard calibration graph (y = 31975x – 704.78, R2 = 0.9998)

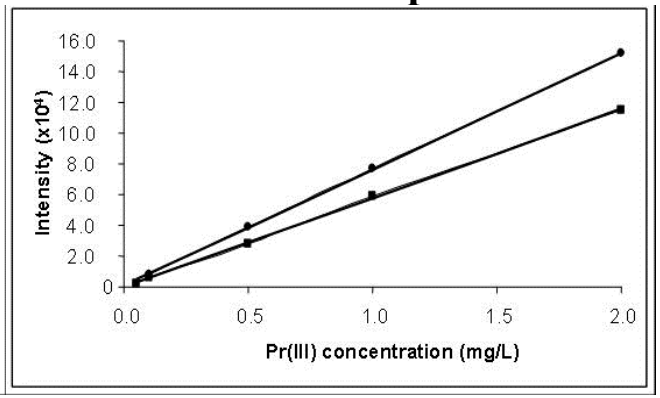

Figure A.2. Calibration graphs for Pr(III). (•) Pr(III) aqueous standard calibration graph (y = 75554x + 747.98, R2 = 1.0000), (■) Pr(III) matrix-matched standard calibration graph (y = 57919x – 111.44, R2 = 0.9997)

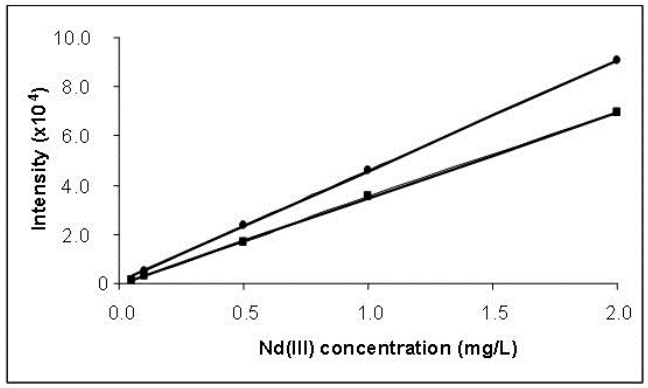

Figure A.3. Calibration graphs for Nd(III). (•) Nd(III) aqueous standard calibration graph (y = 45043x + 654.1, R2 = 0.9999), (■) Nd(III) matrix-matched standard calibration graph (y = 34875x – 268.68, R2 = 0.9998)

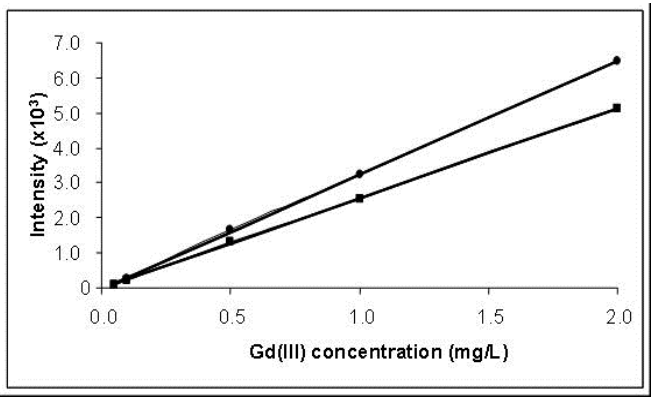

Figure A.4. Calibration graphs for Gd(III). (•) Gd(III) aqueous standard calibration graph (y = 3244.4x – 21.215, R2 = 0.9997), (■) Gd(III) matrix-matched standard calibration graph (y = 2577.8x – 17.176, R2 = 0.9999))

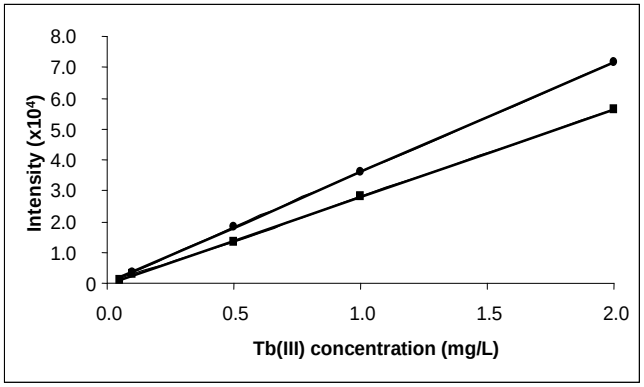

Figure A.5. Calibration graphs for Tb(III). (•) Tb(III) aqueous standard calibration graph (y = 35641x + 267.81, R2 = 1.0000), (■) Tb(III) matrix-matched standard calibration graph (y = 28384x – 271.8, R2 = 0.9999)

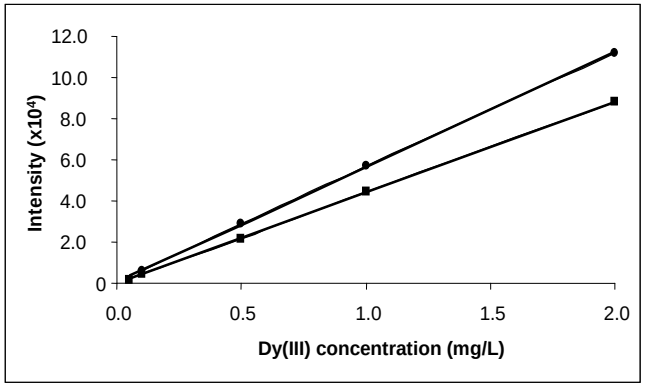

Figure A.6. Calibration graphs for Dy(III). (•) Dy(III) aqueous standard calibration graph (y = 55818x + 734.6, R2 = 0.9999), (■) Dy(III) matrix-matched standard calibration graph (y = 44320x – 304.82, R2 = 0.9999)

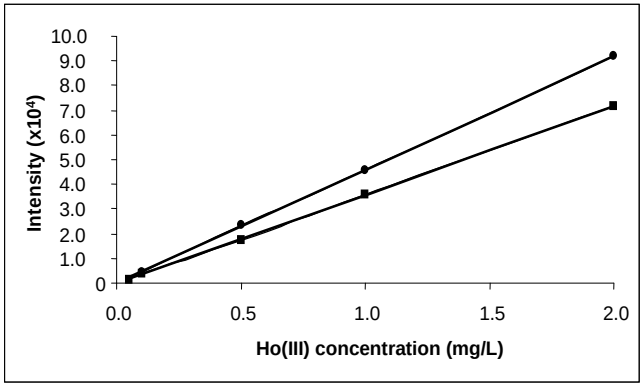

Figure A.7. Calibration graphs for Ho(III). (•) Ho(III) aqueous standard calibration graph (y = 45833x + 51.354, R2 = 0.9999), (■) Ho(III) matrix-matched standard calibration graph (y = 36050x – 225.55, R2 = 0.9999)

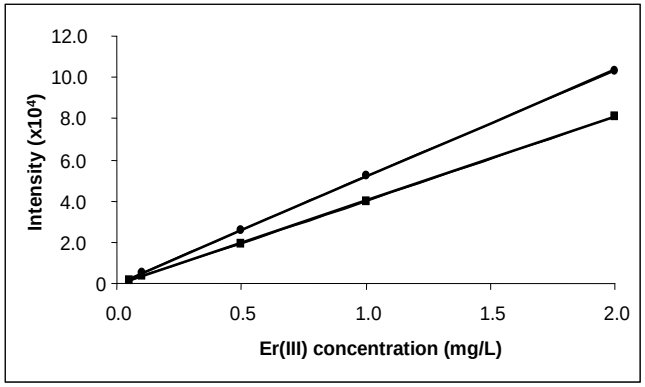

Figure A.8. Calibration graphs for Er(III). (•) Er(III) aqueous standard calibration graph (y = 51781x – 39.998, R2 = 1.0000), (■) Er(III) matrix-matched standard calibration graph (y = 40813x – 737.97, R2 = 0.9998)

APPENDIX B

REEs Sorptions as a Function of pH and Acidity on Different Sorbents

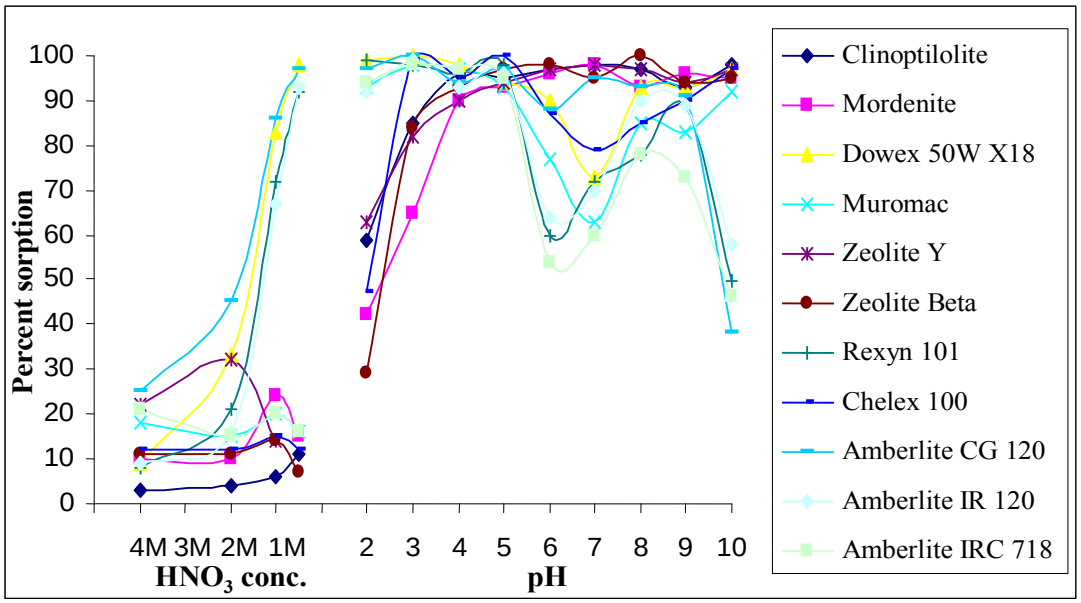

Figure B.1. Cerium sorption as a function of pH and acidity on different sorbents (20.0 mL of 1.0 mg/L solution, sorbent amount: 0.1g)

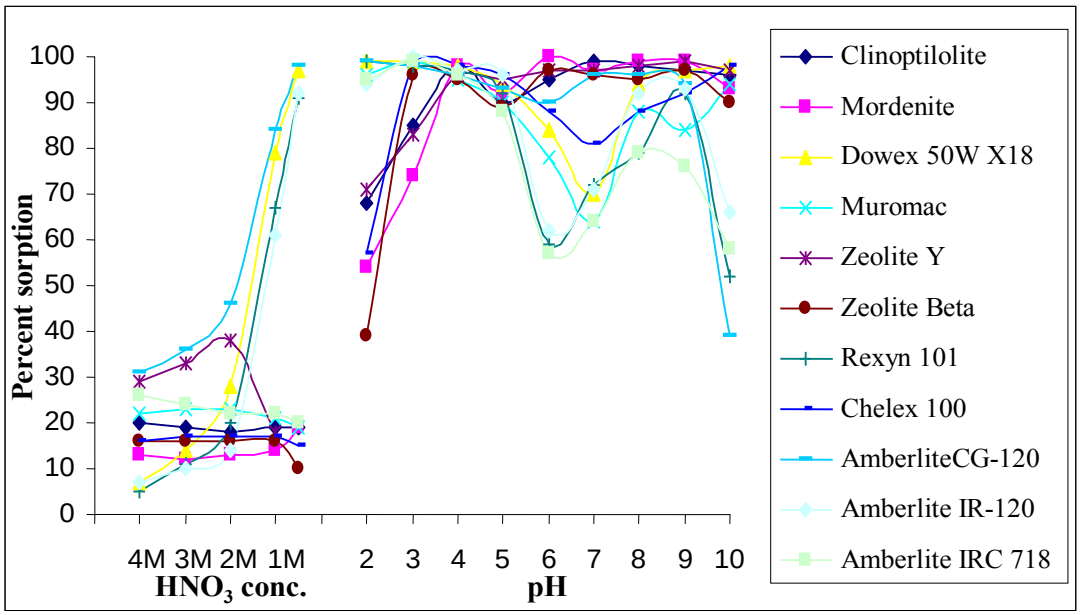

Figure B.2. Praseodymium sorption as a function of pH and acidity on different sorbents (20.0 mL of 1.0 mg/L solution, sorbent amount: 0.1g)

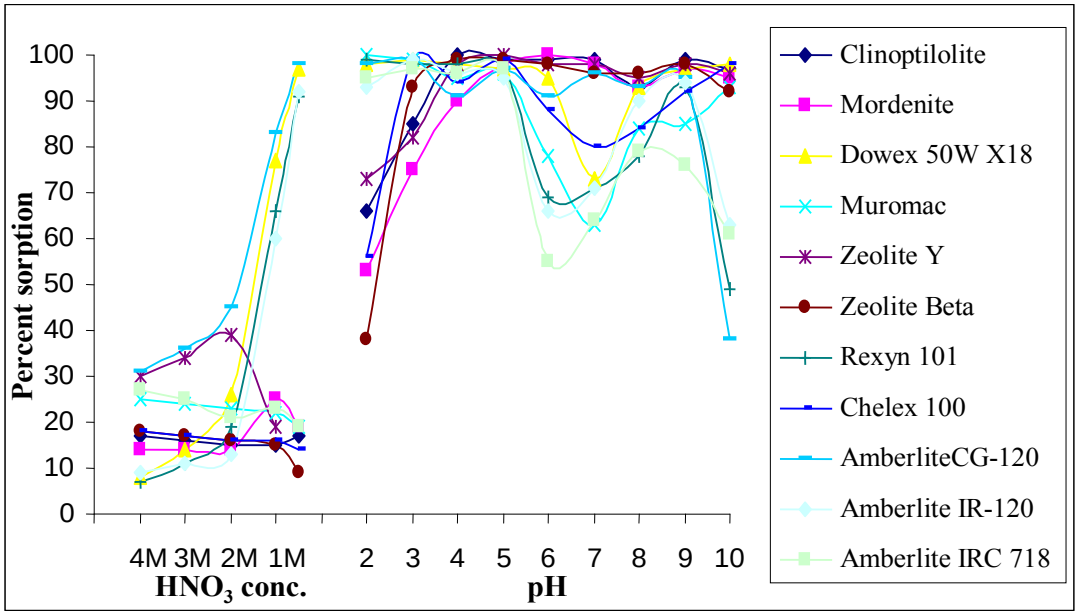

Figure B.3. Neodymium sorption as a function of pH and acidity on different sorbents (20.0 mL of 1.0 mg/L solution, sorbent amount: 0.1g)

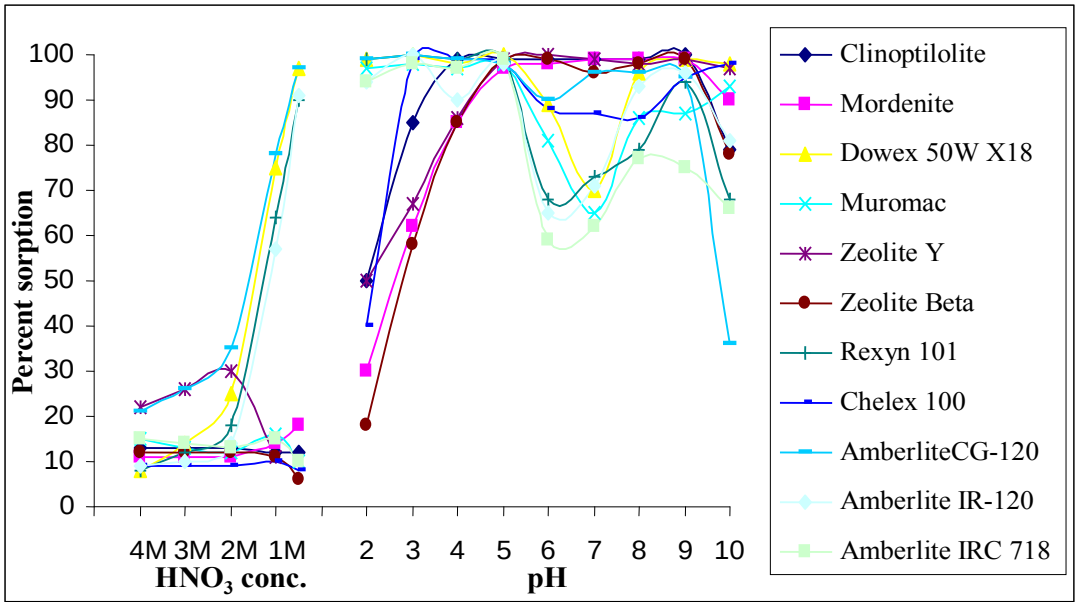

Figure B.4. Gadolinium sorption as a function of pH and acidity on different sorbents (20.0 mL of 1.0 mg/L solution, sorbent amount: 0.1g)

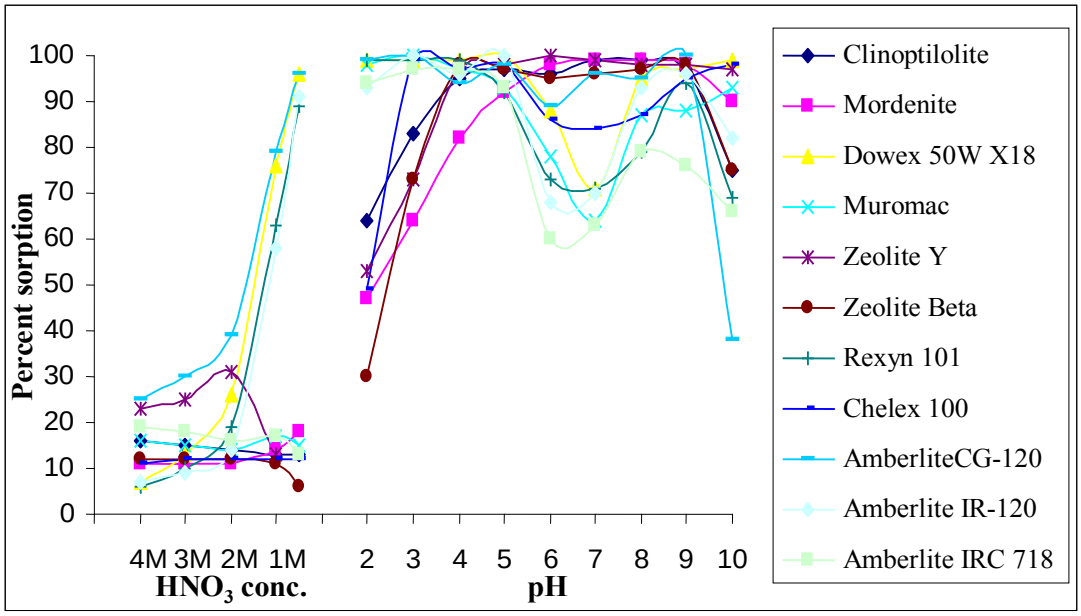

Figure B.5. Terbium sorption as a function of pH and acidity on different sorbents (20.0 mL of 1.0 mg/L solution, sorbent amount: 0.1g)

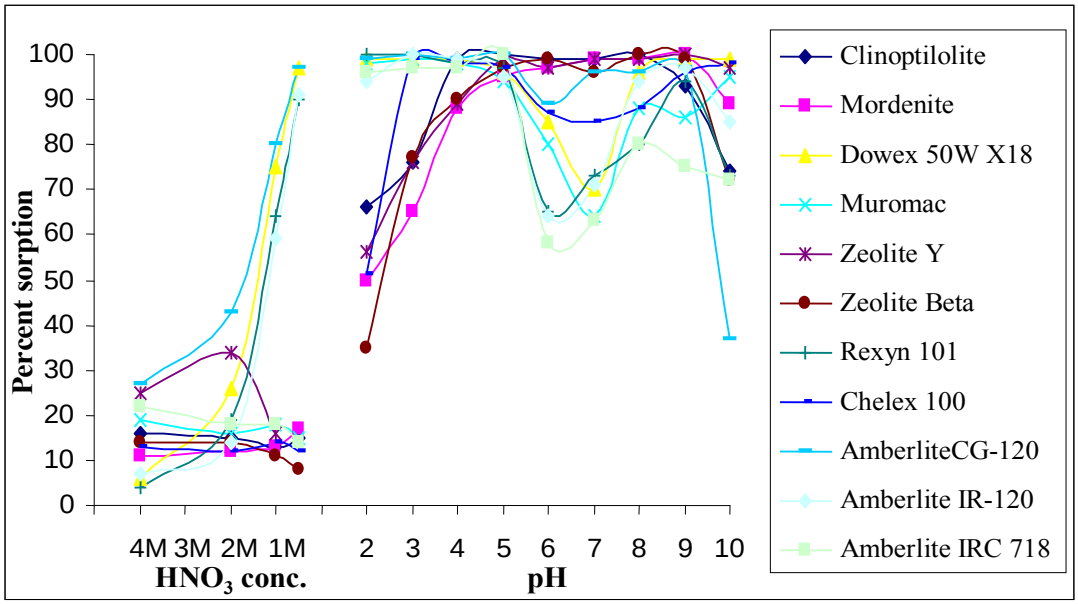

Figure B.6. Dysprosium sorption as a function of pH and acidity on different sorbents (20.0 mL of 1.0 mg/L solution, sorbent amount: 0.1g)

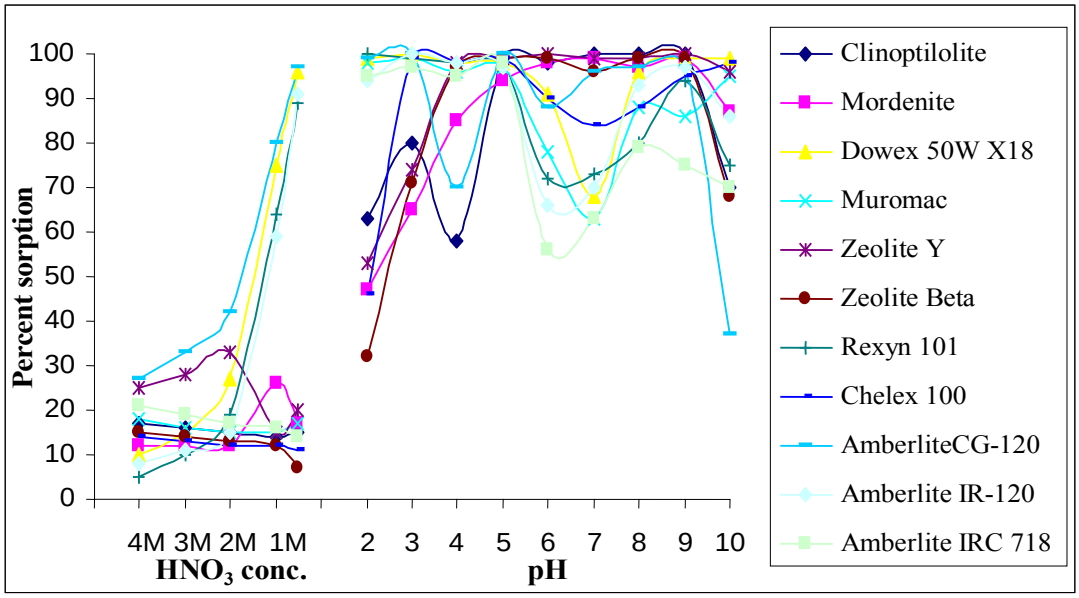

Figure B.7. Holmium sorption as a function of pH and acidity on different sorbents (20.0 mL of 1.0 mg/L solution, sorbent amount: 0.1g)

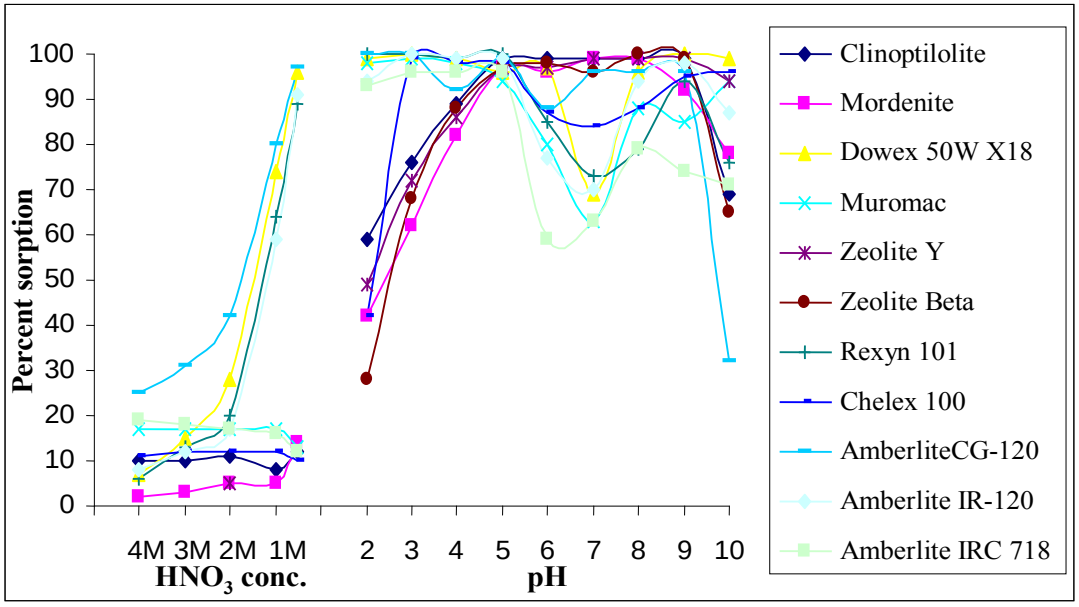

Figure B.8. Erbium sorption as a function of pH and acidity on different sorbents (20.0 mL of 1.0 mg/L solution, sorbent amount: 0.1g)